PHYSICAL REVIEW D **81,** 074027 (2010)

Channel coupling in heavy quarkonia: Energy levels, mixing, widths, and new states

I. V. Danilkin*
Moscow Engineering Physics Institute, Moscow, Russia, and
Institute of Theoretical and Experimental Physics, Moscow, Russia

Yu. A. Simonov†
Institute of Theoretical and Experimental Physics, Moscow, Russia
(Received 13 September 2009; published 23 April 2010)

The mechanism of channel coupling via decay products is used to study energy shifts, level mixing as well as the possibility of new near-threshold resonances in $c\bar{c}$, $b\bar{b}$ systems. The Weinberg eigenvalue method is formulated in the multichannel problems, which allows one to describe coupled-channel resonances and wave functions in a unitary way, and to predict new states due to channel coupling. Realistic wave functions for all single-channel states and decay matrix elements computed earlier are exploited, and no new fitting parameters are involved. Examples of level shifts, widths, and mixings are presented; the dynamical origin of $X(3872)$ and the destiny of the single-channel $2^3P_1(c\bar{c})$ state are clarified. As a result a sharp and narrow peak in the state with quantum numbers $J^{PC} = 1^{++}$ is found at 3.872 GeV, while the single-channel resonance originally around 3.940 GeV becomes increasingly broad and disappears with growing coupling to open channels.

DOI: 10.1103/PhysRevD.81.074027 PACS numbers: 12.39.−x, 13.20.Gd, 13.25.Gv, 14.40.−n

I. INTRODUCTION

Most hadron states are coupled by strong interaction to closed or open decay channels, and thus are subjects of the theory of strongly coupled channels (TSCC). The latter topic was developed during many decades, see [1–5] for a review, and also [6–8] as more recent publications. In the present paper we apply TSCC specifically to the case of Okubo-Zweig-Iizuka rule allowed two-body decay channels of charmonia and bottomonia. In doing so we need several prerequisites. First of all, it is the one-channel description of charmonia and bottomonia as $c\bar{c}$, $b\bar{b}$ states in relativistic Hamiltonian formalism [9], developed in the framework of the field correlator method [10] (see [11] for a review) and wave functions (w.f.) of stable states in x or p space cast in the numerical form. The latter have been accurately computed using this method with only universal input: the string tension σ, the current (pole) quark masses m_i, and the strong coupling $\alpha_s(q)$ [12].

The next ingredient is an effective relativistic Lagrangian for the pair creation, inducing the string breaking. To this end we are using the decay mass vertex $\int \bar{\psi} M_\omega \psi d^4x$ introduced in [13] and exploited for dipion transitions in [13–15] and for the reaction channel $\Upsilon(nS) \to B\bar{B}$, $B\bar{B}\pi$ in [16]. In principle, M_ω can be expressed in terms of quark masses and average energies, but we use it as the only one parameter, which is fixed in our previous studies [13–16] Finally, as shown in [13] and before in [17,18] the transition matrix element reduces to the overlap integral of wave functions of decaying system and products of decay. It is interesting that the vertex operator in this integral contains not only M_ω, but also the Z factor of the decay process constructed from the Dirac trace of all involved hadron vertex states, and projection operators. This technic, introduced in [13], is a relativistic equivalent of the nonrelativistic one with spin-angular momentum (Clebsch-Gordon) coefficients used in the framework of the $^3P_0$ model [19]. As a result one obtains a system of integro-differential equations for new wave functions and energy eigenvalues, which can be easily solved in the lowest approximation for energy shifts, widths, and level mixing coefficients. At the same time we have developed a (2×2) variant of wave functions and matrix elements for light quarks in heavy-light mesons. Several examples of this kind are shown below.

At a deeper level, one meets with several problems: (i) First, the states above decay thresholds are unstable and the definition of the wave function itself is questionable in a rigorous sense, since an admixture of continuous spectrum states appears. Here different approaches exist. The most rigorous is the Weinberg procedure [20], named the Weinberg eigenvalue method (WEM). It is used to define the resonance wave function and energy, as well as the t matrix via Weinberg eigenvalues. The WEM has been used before in the one-channel 2-body and 3-body problems [20,21]. We have found that it is specifically useful in the case of TSCC, since coupled channels (CC) induce the energy-dependent force term, which violates standard orthonormalization procedure, while this term can easily be treated in the WEM. (ii) Second, even the closed channels cause the problems. In terms of hadron loops it

*danilkin@itep.ru
†simonov@itep.ru

was treated in many papers, see e.g. [2] and recent papers [7,8], where some theorems were formulated [7] and the renormalization method was suggested [8].

In essence the problem here is similar to the problem of unquenched quark pairs. It occurs also for stable hadrons, where the renormalozation procedure is necessary in general. We will not discuss these topics in the given paper, assuming that the renormalization is done e.g., by readjusting the pole quark mass. We also disregard the important topic of full relativistic invariance for composite objects moving with different velocities, e.g. charmonium decaying in its c.m. system into heavy-light mesons, with their wave functions defined in their c.m. systems. This is done assuming small relative velocities near thresholds. Far from thresholds these factors become important. Similarly, near thresholds we assume here, as well as in [13–16], the $^3P_0$ type of the decay vertex, while at higher energies this type of decay may be replaced by another one, e.g. the $^3S_1$ type.

In this paper we systematically apply the WEM to find the shifts and widths of (n^3S_1) energy levels, as well as mixing between them. We find the method to be especially useful to discover the analytic structure and pole positions in the case of strong CC. A particular example of the 2^3P_1 level proves to be a good illustration of our analysis. From the experimental point of view two interesting problems appear. The first one, why in experiment only the peak at the lowest $D_0D_0^*$ threshold is seen, while at the slightly higher, $D_+D_-^*$ no peak was ever seen? Secondly, possible resonances at 3.940 GeV found in [22], seemingly are not $J=1$, and very likely the 1^{++} state around 3.940 GeV was never observed. Our analysis allows one to answer both questions at the same time, as will be explained below.

As a result we find two poles due to a single eigenvalue in the positions near 3.872 and 3.940 GeV, but the latter peak becomes too wide and finally disappears with increasing CC, which can explain the experimental situation [22]. Moreover, retaining the peak appears at the lower threshold 3.872 GeV, and not at the higher threshold 3.879 GeV, again in agreement with experiment [22].

The plan of the paper is as follows. In the next section we introduce the general formalism for the Green's functions of charmonia and bottomonia with the inclusion of decay channels. We present equations for wave functions (Green's functions) both in $Q\bar{Q}$ and $(Q\bar{q})(\bar{Q}q)$ channels. In Sec. III the CC resonances are considered in the decay channel and the condition for the existence of a CC resonance is formulated. In Sec. IV the rigorous Weinberg theory of CC resonances is presented. In Sec. V the mixing of states in the WEM is considered. In Sec. VI we present results for values of level shifts and widths for the 3^3S_1 state and also mixing between the 3^3S_1 and 2^3S_1 states, as well as the analysis of the situation in the 2^3P_1 state. In Sec. VII summary and prospectives are given.

II. GENERAL FORMALISM OF STRING-BREAKING CHANNEL COUPLING

We consider two sectors of hidden and open flavor with initial and final bare gauge-invariant operators, for the heavy quarkonium sector:

I. $j_i^{(I)}(x) = \bar{\psi}_Q(x)\Gamma_i\psi_Q(x)$

and for the heavy-light meson sector.

II. $j_i^{(II)}(x) = \bar{\psi}_Q(x)\Gamma_i\psi_q(x)$

where $\Gamma_i = 1, \gamma_\mu, \ldots, D_\mu\sigma_{\mu\nu}, \ldots$. With the help of $j_i^{(I,II)}$ one generates bare mesons and as shown in [13,23] one can project physical amplitudes[1] (Green's functions) with physical wave functions $\Psi_{Q\bar{Q}}^{(n_1)}$, $\psi_{Q\bar{q}}^{(n_2)}$, and $\psi_{\bar{Q}q}^{(n_3)}$. For stationary states one can use Green's functions in energy representation, e.g.

$$G^{(0)}_{Q\bar{Q}}(1,2;E) = \sum_{n_1} \frac{\Psi^{(n_1)}_{Q\bar{Q}}(1)\Psi^{\dagger(n_1)}_{Q\bar{Q}}(2)}{E_{n_1} - E} = \frac{1}{H_0 - E}. \quad (1)$$

Here superscript (0) of Green's function refers to the bare case, when sector II is switched off, and $\Psi^{(n_1)}_{Q\bar{Q}}$, E_{n_1} refer to the eigenfunctions and eigenvalues of the relativistic string Hamiltonian (RSH) H_0 [9]; for the charmonium those were calculated in [12] and for the bottomonium in [25]. In sector II the counterpart of (1) consists of Green's function of the pair $(Q\bar{q})$, $(q\bar{Q})$. We neglect in the first approximation interaction of two color singlet mesons, and write the c.m. Green's function as

$$G^{(0)}_{Qq\bar{q}\bar{Q}}(1\bar{1}|2\bar{2};E) = \sum_{n_2,n_3} \frac{\Psi_{n_2n_3}(1,\bar{1})\Psi^\dagger_{n_2n_3}(2,\bar{2})}{E_{n_2n_3}(\mathbf{p}) - E} d\Gamma(\mathbf{p}). \quad (2)$$

At this point we must take into account a possible transition (decay) of states in sector I into states of sector II, which can be done in several ways. In the literature it is common to assume one of several types of phenomenological decay Lagrangians, e.g. a $^3P_0$ type [19], with vector confinement vertex [1], or with scalar confinement vertex, studied in [18]. For a bottomonium a relativistic string decay vertex of the following form was used in [13–16]:

$$\mathcal{L}_{sd} = \int \bar{\psi}_q M_\omega \psi_q d^4x, \qquad M_\omega = \text{const}, \quad (3)$$

where M_ω was taken to be constant, $M_\omega \approx 0.8$ GeV from decays of the bottomonium into $B\bar{B}$, $B\bar{B}^*$, ... [15,16].

It is important that we work in the c.m. system and consider both wave functions and Hamiltonian obtained in the instantaneous hyperplane, when all time coordinates

[1]Note that the procedure of hadron state projection is here fully equivalent to that used in the lattice approach, see e.g. [24].

of all particles are the same.[2] Therefore the vertex $\mathcal{L}_{sd}$ enters between instantaneous wave functions of $Q\bar{Q}$ on one side and the product of $Q\bar{q}$, $q\bar{Q}$ on another side

$$J_{123} \equiv \frac{1}{\sqrt{N_c}} \int \bar{y}_{123} \Psi^{+}_{Q\bar{Q}} M_\omega \psi_{Q\bar{q}} \psi_{q\bar{Q}} d\tau. \tag{4}$$

At this point one should define exactly how spin, momentum, and coordinate degrees of freedom enter in (4), which we denote by an additional factor $\bar{y}_{123}$ and yet undefined phase space factor $d\tau$. One way is to exploit nonrelativistic-type decomposition which is used in $^3P_0$ calculations [19]. In our considerations we are using two different ways. Below we begin from the fully relativistic formalism of Dirac traces and projection operators, started in [23] for decay constants and in [13] for dipion transitions and then will go into reduced (2×2) spin-tensor formalism, explained in Appendix B. Note that the relativistic formalism with Z factors is similar in lattice calculations for transition matrix elements, see e.g. [24].

In the formalism one considers initial and final meson creation operators I, II, given above [see in Appendix B Table VI of lowest operators and their (2×2) forms], and composes the decay matrix element as shown in Fig. 1 where vertices 1, 2, 3, x are operators $\Gamma_{i=1,2,3,x}$ entering in the bilinears $j_i = \bar{\psi}\Gamma_i\psi$, and lines $(1, 2)$, $(2, x)$, … denote quark Green's functions $S_Q(1, 2)$, $S_{\bar{q}}(2, x)$, etc., so that the matrix element corresponding to Fig. 1 is

$$S(1, 2, x, 3) = \mathrm{tr}\{\Gamma_1 S_Q(1, 2)\Gamma_2 S_{\bar{q}}(2, x)\Gamma_x S_q(x, 3)\Gamma_3 S_{\bar{Q}}(3, 1)\}. \tag{5}$$

As shown in [13,23] in the approximation where one neglects influence of spin forces on wave functions, one can replace

$$S_{Q,q} = \frac{(m_{Q,q} + \omega_{Q,q}\gamma_4 - ip_i^{Q,q}\gamma_i)}{2\omega_{Q,q}} = \Lambda^{+}_{Q,q} G_{Q,q},$$
$$S_{\bar{Q}\,\bar{q}} = \frac{(m_{Q,q} - \omega_{Q,q}\gamma_4 + ip_i^{Q,q}\gamma_i)}{2\omega_{Q,q}} G_{\bar{Q},\bar{q}} = \Lambda^{-}_{Q,q} G_{\bar{Q},\bar{q}}, \tag{6}$$

where $G_{Q,q}$ is the quadratic Green's function, $\Lambda^{\pm}_{Q,q}$ are projection operators, the variables $\omega_{Q,q}$ are the averaged kinetic energies, and $m_{Q,q}$ are the pole masses.

Our physical matrix element corresponding to the decay $\Psi^{(n_1)}_{Q\bar{Q}} \to \psi^{(n_2)}_{Q\bar{q}} \psi^{(n_3)}_{\bar{Q}q}$ can be obtained from (5) by projecting the chosen intermediate states, as shown by dashed lines in Fig. 1.

[2]We omit boost corrections here, which makes the application of our method justifiable only close to thresholds. Far from thresholds one should take into account both boost and, more importantly, a possible change in the pair-creation vertex, since high energy transfer to the $q\bar{q}$ pair might require a gluon-exchange mechanism, hence the $^3S_1$ vertex.

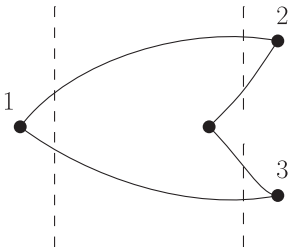

FIG. 1. Decay matrix vertices.

As a result as shown in [13,14] the physical projected matrix element has the form

$$J_{n_1 n_2 n_3}(\mathbf{p}) = \frac{M_\omega}{\sqrt{N_c}} \int \bar{y}_{123} \Psi^{(n_1)}_{Q\bar{Q}}(\mathbf{u} - \mathbf{v}) e^{i\mathbf{pr}} \psi^{(n_2)}_{Q\bar{q}}(\mathbf{u} - \mathbf{x}) \times \psi^{(n_3)}_{\bar{Q}q}(\mathbf{x} - \mathbf{v}) d^3\mathbf{x} d^3(\mathbf{u} - \mathbf{v}), \tag{7}$$

where N_c is the number of colors, $\mathbf{r} = c(\mathbf{u} - \mathbf{v})$, $c = \frac{\omega_Q}{\omega_Q + \omega_q}$ and

$$\bar{y}_{123} = \frac{\bar{Z}_{123}}{\sqrt{\prod_{i=1}^{3} \bar{Z}_i}}.$$

The expressions for $\bar{Z}_{123}$, $\bar{Z}_i$ are proportional to Dirac traces of the projector operators and are given in [13,14]. We point out that the w.f. $\Psi^{(n_1)}_{Q\bar{Q}}$, $\psi^{(n_2)}_{Q\bar{q}}$, $\psi^{(n_3)}_{\bar{Q}q}$ in (7) are no longer full w.f. of mesons, but the radial parts $R^{(n_1)}_{Q\bar{Q}}$, $R^{(n_2)}_{Q\bar{q}}$, $R^{(n_3)}_{\bar{Q}q}$ divided by $\sqrt{4\pi}$, while the angular part of the w.f. is accounted for in the factor $\bar{y}_{123}(\bar{y}^{\mathrm{red}}_{123})$. An important role is played by average values of quark kinetic energies, $\omega_{Q,q} = \langle\sqrt{m^2_{Q,q} + \mathbf{p}^2}\rangle$ inside heavy-light mesons in their c.m. systems (if one neglects c.m. motion of these mesons). The numbers of ω_Q, ω_q are computed from the relativistic string Hamiltonian in [12,25]. In practical calculations it is more useful to exploit the (2×2) reduction of the bispinor wave functions in (4), as $\psi = \binom{v}{w}$and $\bar{\psi}\Gamma\psi = (v^c, w^c)\gamma_2\gamma_4\Gamma\binom{v}{w}$; see details in Appendix B. The resulting matrix element has the same form as in (7) but with $M_\omega \bar{y}_{123} \to \gamma \bar{y}^{\mathrm{red}}_{123}$, where $\bar{y}^{\mathrm{red}}_{123}$ is given in Table VII and γ is proportional M_ω (see Appendix C).

Now one can define the self-energy part in sector I due to sector II in the intermediate state, which is

$$w_{nm}(E) = \int \frac{d^3\mathbf{p}}{(2\pi)^3} \sum_{n_2 n_3} \frac{J_{nn_2n_3}(\mathbf{p}) J^{+}_{mn_2n_3}(\mathbf{p})}{E - E_{n_2n_3}(\mathbf{p})}, \tag{8}$$

and the total Green's function in sector I can be written as (sum over bound states only)

$$G^{(I)}_{Q\bar{Q}}(1,2;E) = \sum_n \frac{\Psi^{(n)}_{Q\bar{Q}}(1)\Psi^{+(n)}_{Q\bar{Q}}(2)}{E_n - E} - \sum_{n,m} \frac{\Psi^{(n)}_{Q\bar{Q}}(1) w_{nm}(E) \Psi^{+(m)}_{Q\bar{Q}}(2)}{(E_n - E)(E_m - E)} + \cdots, \tag{9}$$

where the ellipsis implies terms of higher order in w_{nm} and this can be summed up as

$$G^{(I)}_{Q\bar{Q}}(1,2;E) = \sum_{n,m} \Psi^{(n)}_{Q\bar{Q}}(1)(\hat{E} - E + \hat{w})^{-1}_{nm} \Psi^{+(m)}_{Q\bar{Q}}(2), \tag{10}$$

where matrix $(\hat{E})_{nm} = E_n \delta_{nm}$.

Note, that in (10) the Green's function is actually a projection of the coupled-channel system on the original unperturbed $Q\bar{Q}$ wave functions $\Psi^{(n)}_{Q\bar{Q}}$. In reality wave functions of the coupled-channel system differ from the latter and acquire continuous spectrum pieces above the decay threshold, and hence need a special treatment to be discussed below.

The new spectrum is obtained from (10) as

$$\det(E - \hat{E} - \hat{w}) = 0, \tag{11}$$

for one level in sector I it simplifies

$$E = E_n + w_{nn}(E), \tag{12}$$

which yields energy shift and width in the first order approximation in $\hat{w}$:

$$E^{(1)}_n = E_n + \mathrm{Re}(w_{nn}(E_n)), \qquad \Gamma^{(1)}_n = 2\mathrm{Im}(w_{nn}(E_n)). \tag{13}$$

In the next order one should solve the transcendental in E one-channel Eq. (12), which is valid when w_{nn} is large, but $|w_{nm}| \ll |E_n - E_m|$.

Below the decay threshold one can diagonalize the matrix in (10) with unitary matrices

$$((E - \hat{E} - \hat{w})^{-1})_{nm} = U^+_{n\lambda}(E) \frac{1}{E - E_\lambda} U_{\lambda m}(E) \tag{14}$$

and the Green's function acquires the form

$$G^{(I)}_{Q\bar{Q}} = \sum_\lambda \Phi_\lambda \frac{1}{E_\lambda - E} \Phi^+_\lambda, \qquad \Phi_\lambda = \sum_n \Psi^{(n)}_{Q\bar{Q}} U^+_{n\lambda}(E). \tag{15}$$

In this way Φ_η become new orthogonal states comprising all effects of mixture between bound states due to closed channels. The same procedure can be applied for open channels (above the decay threshold) when one neglects the widths of the levels, i.e. imaginary part of $\hat{w}$.

One can define interaction V_{121} in sector I due to sector II,

$$V_{121}(\mathbf{r}, \mathbf{r}') = \sum_{n_2 n_3} G^{(0)}_{n_2 n_3}(\mathbf{r} - \mathbf{r}') X_{n_2 n_3}(\mathbf{r}) X^+_{n_2 n_3}(\mathbf{r}'), \tag{16}$$

with

$$G^{(0)}_{n_2 n_3}(\mathbf{r} - \mathbf{r}') = \int \frac{d^3\mathbf{p}}{(2\pi)^3} \frac{e^{i\mathbf{p}(\mathbf{r}-\mathbf{r}')}}{E_{n_2 n_3}(\mathbf{p}) - E}, \tag{17}$$

$$X_{n_2 n_3}(\mathbf{r}) = \frac{M_\omega}{\sqrt{N_c}} \int \frac{d^3\mathbf{q}}{(2\pi)^3} e^{i\mathbf{q}\mathbf{r}} \psi^{(n_2)}_{Q\bar{q}}(\mathbf{q}) \psi^{(n_3)}_{\bar{Q}q}(\mathbf{q}), \tag{18}$$

or, in momentum space

$$V_{121}(\mathbf{q}, \mathbf{q}') = \sum_{n_2 n_3} \int \frac{d^3\mathbf{p}}{(2\pi)^3} \frac{X_{n_2 n_3}(\mathbf{q} - \mathbf{p}) X^+_{n_2 n_3}(\mathbf{q}' - \mathbf{p})}{E - E_{n_2 n_3}(\mathbf{p})}, \tag{19}$$

where

$$X_{n_2 n_3}(\mathbf{Q}) = \frac{M_\omega}{\sqrt{N_c}} \psi^{(n_2)}_{Q\bar{q}}(\mathbf{Q}) \psi^{(n_3)}_{\bar{Q}q}(\mathbf{Q}).$$

Now the one-channel Hamiltonian H_0 in sector I is augmented by the term V_{121},

$$H = H_0 + V_{121}, \qquad H\Psi_{n_1} = E\Psi_{n_1}. \tag{20}$$

Note, that the CC interaction can be strong enough to support its own bound states, as was studied in [5], where this type of resonances was called the CC resonances.

Let us now turn to the RSH H_0, derived from the gauge-invariant meson Green's function in QCD in the one-channel case in [9]. This Hamiltonian has been successfully applied to light mesons [26], heavy-light mesons [23,27], and heavy quarkonia [12,25] and has a simple form:

$$H_0 = \frac{\omega_1}{2} + \frac{\omega_2}{2} + \frac{m_1^2}{2\omega_1} + \frac{m_2^2}{2\omega_2} + \frac{\mathbf{p}^2}{2\omega_{\mathrm{red}}} + V_{11}(r), \tag{21}$$

$$V_{11}(r) = V_B(r) + V_{SD}(r, \omega_i). \tag{22}$$

In general, the quantity ω_i appearing in this expression is an operator, which in the so-called einbein approximation is defined by an extremum condition $\frac{\partial M}{\partial \omega_i} = 0$. A simple expression for the spin-averaged mass $M(nl)$ follows from the RSH (21)

$$M(nl) = \frac{\omega_1}{2} + \frac{\omega_2}{2} + \frac{m_1^2}{2\omega_1} + \frac{m_2^2}{2\omega_2} + E_{nl}(\omega_{\mathrm{red}}). \tag{23}$$

Here, the excitation energy $E_{nl}(\omega_{\mathrm{red}})$ depends on the reduced mass $\omega_{\mathrm{red}} = \frac{\omega_1\omega_2}{\omega_1+\omega_2}$. The formula (23) does not contain any additive constant; for a light quark (e.g. in the D meson) a negative (not small) nonperturbative self-energy term appears, proportional to $(\omega_u)^{-1}$; it has to be added to their masses [28]. In the case of charmonium this term is small; the variables $\omega_i(nl)$, the excitation energy $E_{nl}(\omega_{\mathrm{red}})$, and the w.f. are calculated from the Hamiltonian

(21) and two extremum conditions $\partial M(nS)/\partial\omega_i = 0$ ($i = 1, 2$), [9,29]:

$$H_0\varphi_{nl}(r) = M(nl)\varphi_{nl}(r),$$
$$\omega_i^2(nl) = m_i^2 - \frac{2\omega_i^2(nl)\partial E(nl, \omega_{\rm red})}{\partial\omega_i(nl)}, \qquad (i = 1, 2). \tag{24}$$

The potential $V_B(r)$ in (22) is derived in the framework of the field correlator method [10–12] and is the sum of a pure scalar confining term and a gluon-exchange part,

$$V_B(r) = \sigma r - \frac{4}{3}\frac{\alpha_B(r)}{r}, \tag{25}$$

where the vector coupling $\alpha_B(r)$ is taken in the two-loop approximation and possesses two important features: the asymptotic freedom behavior at small distances, defined by the QCD constant $\Lambda_B(n_f)$ [which is considered to be known, because Λ_B is directly expressed via the QCD constant $\Lambda_{\overline{\rm MS}}(n_f)$ in the $\overline{\rm MS}$ renormalization scheme]; it freezes at large distances. Details about the effective fine-structure constant can be found in Ref. [12].

III. RESONANCES IN THE DECAY SECTOR

As discussed in [5], the situation of two coupled sectors I, II, $Q\bar{Q}$ and $(Q\bar{q})(\bar{Q}q)$, can be treated in two ways:

(1) as a coupled system of matrix Green's functions,

$$G^{ab}, \qquad a, b = I, II;$$

(2) as a reduction of the two-sector problem to the one-sector problem with energy-dependent "potential" V_{121} or V_{212}.[3] We shall continue our one-channel treatment from the point of view of sector II. In the same way as it was done before, one can define the potential $V_{212} \equiv V_{n_2n_3,n_2'n_3'}$

$$V_{n_2n_3,n_2'n_3'}(\mathbf{p}, \mathbf{p}', E) = \sum_n \frac{J^+_{nn_2n_3}(\mathbf{p})J_{nn_2'n_3'}(\mathbf{p}')}{E - E_n}. \tag{26}$$

Defining also

$$J_{nn_2n_3}(\mathbf{r}) \equiv \int \frac{d^3\mathbf{p}}{(2\pi)^3} e^{i\mathbf{pr}} J_{nn_2n_3}(\mathbf{p}),$$

one can write

$$V_{n_2n_3,n_2'n_3'}(\mathbf{r}, \mathbf{r}', E) = \sum_n \frac{J^+_{nn_2n_3}(\mathbf{r})J_{nn_2'n_3'}(\mathbf{r}')}{E - E_n} \tag{27}$$

[3]Note that a parallel treatment of the open channel problem in nuclear reactions is developed by Feshbach with the help of the projection operators in his unified theory of nuclear reactions [30].

and as a result one obtains a system of equations in sector II

$$(H_0 + V_{22}(\mathbf{r}))\psi_{n_2n_3}(\mathbf{r}) + \int V_{n_2n_3,n_2'n_3'}(\mathbf{r}, \mathbf{r}', E)\psi_{n_2'n_3'}(\mathbf{r}')d^3\mathbf{r}' = E\psi_{n_2n_3}(\mathbf{r}), \tag{28}$$

where $V_{22}(\mathbf{r})$ is a direct interaction between two color singlet mesons, which we neglect in the first approximation, and H_0 is the same as in (21) but for m_1, m_2 equal to masses of mesons with quantum numbers n_2, n_3, $H_0 = H_0(n_2n_3)$. Neglecting V_{22}, one can easily rewrite (28) for the separable interaction (27)

$$\psi_{n_2n_3}(\mathbf{r}) = -\sum_n \int d^3\mathbf{r}' d^3\mathbf{r}'' G^{(0)}_{n_2n_3}(\mathbf{r}, \mathbf{r}') \times \frac{J^+_{nn_2n_3}(\mathbf{r}')J_{nn_2'n_3'}(\mathbf{r}'')}{E - E_n}\psi_{n_2'n_3'}(\mathbf{r}''), \tag{29}$$

where

$$G^{(0)}_{n_2n_3}(\mathbf{r}, \mathbf{r}') = \int \frac{d^3\mathbf{k}}{(2\pi)^3}\frac{e^{i\mathbf{k}(\mathbf{r}-\mathbf{r}')}}{H_0^{(n_2n_3)}(\mathbf{k}) - E}. \tag{30}$$

Introducing $\varphi_n \equiv \int J_{nn_2n_3}(\mathbf{r})\psi_{n_2n_3}(\mathbf{r})d^3\mathbf{r}$, and integrating both sides of (29) with $J_{mn_2n_3}(\mathbf{r})d\mathbf{r}$, one has from (29)

$$\varphi_m = \sum_n \frac{w_{mn}(E)\varphi_n}{E - E_n} \tag{31}$$

with the same $w_{mn}(E)$ as in (8), and the equation for eigenvalues is again (11).

Since the CC interaction (27) is separable, one can study the structure of the spectrum of our CC problem in more detail; in particular, whether there can appear poles (CC resonances in terminology of [5]) due to strong CC interaction, which are additional to the one-sector spectrum of poles E_n, the latter being simply shifted by CC. As was argued in [5], we define the integral

$$I_{n_2n_3}(E) = \left| \int \frac{d^3\mathbf{p}}{(2\pi)^3}\sum_n \frac{|J_{nn_2n_3}(\mathbf{p})|^2}{(E - E_n)(H_0^{(n_2n_3)}(\mathbf{p}) - E)} \right|. \tag{32}$$

According to [5], a bound state in a single channel n_2n_3 due to CC with the sector I can exist, if in the region, where (32) is real [below threshold $E_{\rm th}(n_2, n_3)$], it becomes larger than 1

$$I_{n_2n_3}(E) > 1, \qquad E < E_{\rm th}(n_2, n_3). \tag{33}$$

In the momentum space one has

$$\tilde{H}_0(\mathbf{p})\psi_{n_2n_3}(\mathbf{p}) + \int V_{n_2n_3,n_2'n_3'}(\mathbf{p}, \mathbf{p}', E)\psi_{n_2'n_3'}(\mathbf{p}')\frac{d^3\mathbf{p}'}{(2\pi)^3} = E\psi_{n_2n_3}(\mathbf{p}), \tag{34}$$

which yields the same equation as in (31). As before in

Eq. (11), one obtains from (34) the equation $\det(E - \hat{E}_n - \hat{w}) = 0$, which defines all poles in the cut E plane below thresholds and on the second, and higher Riemann sheets.

IV. THEORY OF COUPLED-CHANNEL RESONANCES BASED ON THE WEINBERG EIGENVALUE METHOD

The coupled-channel problem can be quantified using the eigenvalue analysis introduced by Weinberg [20]. Although this formalism has been developed long ago, it is still not widely known. That is why in this section we present a short summary of corresponding formulas leaving details to Appendix D.

The Schrödinger equation for two-body like Hamiltonian $H = H_0 + V$ can be written in the standard (time-independent) way

$$(H_0 - E)\Psi_E(r) = -V\Psi_E(r), \tag{35}$$

where E is a spectral variable, $\Psi_E(r)$ is an energy eigenstate, and V is an operator, which in the nonlocal case acts in (35) as $V(\Psi_E(\mathbf{r})) = \int V(\mathbf{r}, \mathbf{r}')\Psi_E(\mathbf{r}')d\mathbf{r}'$. In the Weinberg method, instead, w.f. are the eigensolutions of

$$(H_0 - E)\Psi_\nu(r, E) = \frac{-V}{\eta_\nu(E)}\Psi_\nu(r, E), \tag{36}$$

where E is the continuous parameter entering w.f. and the index ν labels the discrete eigenvalues and eigenvectors. The Weinberg eigenvalue $\eta_\nu(E)$ is the potential scale and thus the spectrum consists of all the potential rescalings that give solution to that equation, for given energy E.

Let us now turn to the question of the rigorous definition of the resonance wave function and start with the one-state situation, when only one state is considered in sector II, with fixed n_2, n_3. The induced interaction $V_{212}(\mathbf{r}, \mathbf{r}', E)$ has the form (27) and direct interaction V_{22} is neglected for simplicity. One can exploit the WEM [20], and divide the potential $V_{212}(\mathbf{r}, \mathbf{r}', E)$ in (32) by an energy-dependent factor $\eta_\nu(E)$ considering instead of Eq. (28) another one (with $V_{22} \equiv 0$)

$$H_0\Psi_\nu(\mathbf{r}, E) + \int \frac{V_{212}(\mathbf{r}, \mathbf{r}', E)}{\eta_\nu(E)}\Psi_\nu(\mathbf{r}', E)d^3\mathbf{r}' = E\Psi_\nu(\mathbf{r}, E), \tag{37}$$

which defines for each E the eigenvalue $\eta_\nu(E)$ and eigenfunction $\Psi_\nu(r, E)$, with the boundary conditions

$$\Psi_\nu(0) = \text{const}, \qquad \Psi_\nu(r \to \infty) = C\frac{e^{ikr}}{r}, \qquad k = \sqrt{2\tilde{M}(E - E_{\text{th}})}. \tag{38}$$

For $E < E_{\text{th}}$ one has instead $\Psi_\nu(r \to \infty) \sim c\exp(-\kappa r)/r$. In the WEM, resonance structures as well as bound sates can be obtained in terms of Weinberg eigenvalues $\eta_\nu(E)$. Note that a solution of integro-differential equation (37) in the coordinate space can satisfy these boundary conditions for each energy E only for some discrete value of $\eta_\nu(E)$, $\nu = 1, 2, \ldots$. Compare e.g. with the case of bound states (energy below threshold), where boundary conditions at origin and infinity can be matched only for discrete energy E_i in standard formalism ($\eta = 1$) or at some $\eta_i(E)$ for any E in WEM, with the relation $\eta_i(E_i) = 1$.

The normalization of wave functions is

$$\int d\mathbf{r}d\mathbf{r}'\Psi_\nu(\mathbf{r}, E)\hat{V}_{212}(\mathbf{r}, \mathbf{r}', E)\Psi_{\nu'}(\mathbf{r}, E) = -\delta_{\nu\nu'}\eta_\nu(E). \tag{39}$$

Note that $\hat{V}_{212}(E)$ is real analytic (holomorphic) for all E except for pole positions, and the off-shell t matrix looks as (see [20] and Appendix D for a derivation)

$$t(\mathbf{p}, \mathbf{p}', E) = -\sum_\nu \frac{\eta_\nu(E)}{1 - \eta_\nu(E)}a_\nu(\mathbf{p}, E)a_\nu(\mathbf{p}', E), \tag{40}$$

with

$$a_\nu(\mathbf{p}, E) = (H_0(\mathbf{p}) - E)\Psi_\nu(\mathbf{p}, E), \tag{41}$$

$$\int \frac{a_\nu(\mathbf{p}, E)a_{\nu'}(\mathbf{p}, E)}{H_0(\mathbf{p}) - E}\frac{d^3\mathbf{p}}{(2\pi)^3} = \delta_{\nu\nu'}, \tag{42}$$

and the Green's function (10) has the form

$$G^{(I)}_{Q\bar{Q}}(1, 2; E) = \sum_\nu \frac{\Psi_\nu(1, E)\Psi^+_\nu(2, E)}{1 - \eta_\nu(E)}. \tag{43}$$

The sum over ν is fast converging as one can see from the example of square well and other potentials fast decreasing at ∞ [21]. Therefore in what follows in our calculations we shall consider only one term in the sum over ν, which is relevant for a given threshold.

The Breit-Wigner resonances in sector II are obtained from the condition that for some $\nu = \nu_0$, $\eta_{\nu_0}(E_0 - \frac{i\Gamma}{2}) = 1$, and

$$\eta_{\nu_0}(E) = 1 + \eta'_{\nu_0}\left(E_0 - \frac{i\Gamma}{2}\right)\left(E - E_0 + \frac{i\Gamma}{2}\right) + \cdots. \tag{44}$$

Note that the corresponding $\Psi_{\nu_0}(r, E)$ serves as the normalized resonance wave function and can be used e.g. to calculate average values of some operator or perturbative shift of resonance position. The $Q\bar{Q}$ Green's function with account of channel coupling can be written near the pole $E = E^R$ (resonance) as

$$G^{(I)}_{Q\bar{Q}}(1, 2; E) = \frac{\bar{\Psi}_\nu(1, E)\bar{\Psi}^+_\nu(2, E)}{E^R - E}, \qquad \bar{\Psi}_\nu = \frac{\Psi_\nu}{\sqrt{\frac{d\eta_\nu(E^R)}{dE}}}. \tag{45}$$

As seen from (37), the introduction of WEM eigenvalue in equations reduces to the replacement $w_{mn}(E) \to \frac{w_{mn}(E)}{\eta(E)}$,

hence the resulting equation for the calculation of $\eta(E)$ is

$$\det\left(\hat{1} - \frac{\hat{w}(E)}{\eta(E)}\frac{1}{E-\hat{E}}\right) = 0, \qquad (\hat{E})_{mn} = E_n\delta_{mn}. \quad (46)$$

Equation (46) is of the nth power in η, when n levels $(Q\bar{Q})$ are taken into account, and this yields n roots $\eta_k(E)$, $k = 1, \ldots, n$. The total number of poles is given by solutions $\eta_k(E_l) = 1$, $l = 1, \ldots, N_p$, where N_p depends on behavior of $\eta_k(E)$.

We started formally with the one channel in sector II, i.e. with fixed n_2, n_3, hence in $\hat{w}(E)$ in Eq. (46) the sum over n_2, n_3 [cf. Eq. (8)] reduces to one term. However, for several states n_2, n_3 one has Eq. (28) with interaction kernel $\hat{V}_{212}$ as a matrix in indices n_2, n_3, n_2', n_3', and if $\eta(E)$ in (37) does not depend on n_2, n_3, then as a result one has for $\eta(E)$ the same Eq. (46), but now with $\hat{w}(E)$, which corresponds fully to (8), i.e. contains the sum over n_2, n_3.

Let us discuss how the basic equation (46) changes for many channels n_2, n_3. We start with Eq. (29), which is equivalent to (37), when one introduces in (29) in the denominator on the right-hand side the factor $\eta_\nu(E)$. Multiplying both sides of this modified Eq. (29) with $J_{mn_2n_3}(\mathbf{r})$ and integrating and summing over n_2, n_3 one obtains an equation similar to (31)

$$\varphi_m^\nu(E) = \frac{1}{\eta_\nu(E)}\sum_n \frac{w_{mn}(E)\varphi_n^\nu(E)}{E-E_n}, \qquad (47)$$

where $\varphi_m(E) = \sum_{n_2n_3} J_{mn_2n_3}(\mathbf{r})\psi_{n_2n_3}(\mathbf{r})d^3\mathbf{r}$, and $w_{mn}(E)$ is the same, as in (8), i.e. again with the sum over n_2, n_3. The resulting equation to determine $\eta(E)$ is again (46), and all equations (37)–(39) have the same form, if one takes into account that Ψ_ν is a column of $\psi_{n_2n_3}$ components and $\hat{V}_{212}$ is a matrix in indices n_2n_3, $n_2'n_3'$.

Finally, the separate components $\psi_{n_2n_3}$ are found through $\varphi_n(E)$ via [cf. (29)]

$$\psi_{n_2n_3}(\mathbf{r}) = -\sum_n \frac{\varphi_n^\nu(E)}{\eta_\nu(E)(E-E_n)} \times \int G^{(0)}_{n_2n_3}(\mathbf{r},\mathbf{r}')J^+_{nn_2n_3}(\mathbf{r}')d\mathbf{r}', \qquad (48)$$

and partial widths of the resonance are found in lowest approximation as (for one-channel n in sector I)

$$\Gamma_{nn_2n_3}(E^R) = 2\,\mathrm{Im}_{n_2n_3}(w_{nn}(E^R)) = 2\pi\int\frac{d^3\mathbf{p}}{(2\pi)^3}|J_{nn_2n_3}(\mathbf{p})|^2\delta(E^R - E_{n_2n_3}(\mathbf{p})). \qquad (49)$$

To understand the possible origin and position of resonances in our CC problems, one can consider several typical cases, depending on relative positions of bare resonances E_n and thresholds $E_{\mathrm{th}}(n_2n_3)$. Consider first one state in sector I, one state in sector II, then $w_{nn}(E) < 0$ for $E < E_{\mathrm{th}}$, and $\mathrm{Re}(w_{nn}(E))$ changes sign at $E = E^*$. The resulting qualitative picture of $\eta(E) = \frac{w_{nn}(E)}{E-E_n}$ is shown in Fig. 2 for three cases: $E_n < E_{\mathrm{th}}$ [Fig. 2(a)]; $E_{\mathrm{th}} < E_n < E^*$ [Figs. 2(b) and 2(d)]; $E_n > E^*$ [Fig. 2(c)]. In Figs. 2(a) and 2(b) one can see one critical energy for which $\eta(E) = 1$. This point corresponds to the shifted energy level E_n.

Note the possibility of a pair of additional roots of equation $\eta(E) = 1$, when $E_n > E^*$, $E_{\mathrm{th}} < E_n < E^*$, and

$$w_{nn}(E_{\mathrm{th}}) > |E_n - E_{\mathrm{th}}|. \qquad (50)$$

The condition (50) defines the strength of CC interaction in the situation depicted in Figs. 2(c) and 2(d) which is necessary one additional pole near the threshold energy (see Appendix E for details). As we shall show below in Sec. VI, the situation of Fig. 2(d) is most likely realized in the $^3P_1$ state of charmonium, where the threshold peak corresponds to the $X(3872)$ state. In this case actually two close-by thresholds are present ($D_0D_0^*$ and $D_+D_-^*$), and as will be seen, the experimentally observed situation with one peak at lowest threshold and wide structure near $E \sim 3.940$ GeV indeed occurs.

Consider now the case of two levels in sector I, E_1 and E_2; and one (or more) state in sector II. The equation for $\eta(E)$ has the form

$$\eta^2(E) - \eta(E)(\tilde{w}_{11} + \tilde{w}_{22}) - \tilde{w}_{12}\tilde{w}_{21} = 0, \qquad (51)$$

with $\tilde{w}_{ik} \equiv \frac{w_{ik}(E)}{E-E_k}$, and the result

$$\eta_\pm(E) = \tfrac{1}{2}(\tilde{w}_{11} + \tilde{w}_{22}) \pm \tfrac{1}{2}\sqrt{(\tilde{w}_{11} - \tilde{w}_{22})^2 + 4\tilde{w}_{12}\tilde{w}_{21}}, \qquad (52)$$

where for notational convenience we have suppressed the energy dependence of the $\tilde{w}_{nm}$.

Near $E = E_1$, $\eta_\pm(E)$ can be identified with the one-channel eigenvalues $\eta_1(E) \equiv \frac{w_{11}(E)}{E-E_1}$ and $\eta_2(E) = \frac{w_{22}(E)}{E-E_2}$, namely, for $E < E_1$ and $E \to E_1$ one has

$$\eta_+(E \to E_1) = \eta_1(E) + \frac{w_{12}(E)w_{21}(E)}{w_{11}(E)(E-E_2)} + \cdots, \qquad (53)$$

$$\eta_-(E \to E_1) = \eta_2(E) - \frac{w_{12}(E)w_{21}(E)}{w_{11}(E)(E-E_2)}, \qquad (54)$$

and for $E \to E_2$ one should change in (53) and (54) $1 \leftrightarrow 2$.

The situation with trajectories $\eta_\pm(E)$ is in general rather complicated, and we describe below only one case when $E_1 < E_2 < E_{ik}^*$, $i, k = 1, 2$ where $\mathrm{Re}(w_{ik}(E_{ik}^*)) = 0$, and in the case of strong mixing of channels 1 and 2 the point E_0, where $\mathrm{Re}(\eta_+(E_0)) = \mathrm{Re}(\eta_-(E_0))$ lies between E_1 and E_2. (The position of E_{th} is irrelevant for the situation where all imaginary parts are neglected.) However for weak mixing of channels 1, 2 roots η_+, η_- never coincide. One can see from (52) that in the weak mixing case only two poles remain, corresponding to shifted levels E_1, E_2 and no new resonances appear at least for $E < E_{ik}^*$.

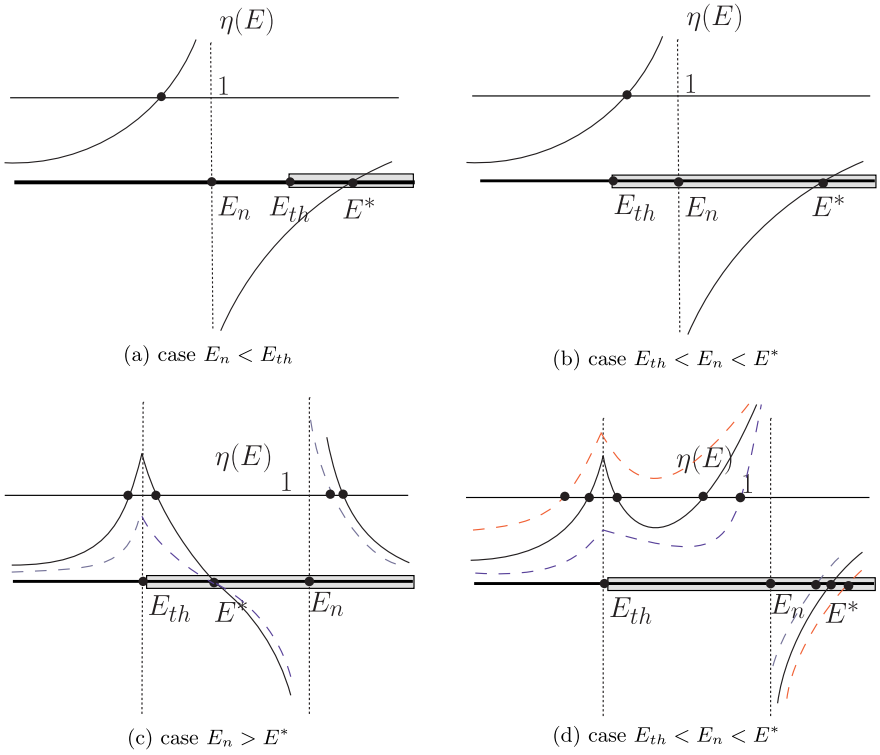

FIG. 2 (color online). Qualitative pictures of Weinberg eigenvalues $\mathrm{Re}(\eta(E))$ as a function of energy E, where E_n is the eigenvalue of the single-channel relativistic string Hamiltonian H_0 (bare resonance), E_{th} denotes threshold, and E^* is the point, where $\mathrm{Re}(w_{nn}(E))$ changes sign.

V. MIXING OF STATES IN THE WEINBERG FORMALISM

The WEM solves the important problem of constructing the full set of orthogonal states in the coupled-channel problem, and thus the problem of mixing of states. This is nontrivial in the situation under investigation, since the interaction in sector I induced by the coupling to sector II, $V_{121}(\mathbf{r}, \mathbf{r}')$, Eq. (16), is energy dependent and hence violates the orthogonality of eigenstates. In addition, for energies above threshold, this interaction is complex and makes the corresponding states the resonances, which cannot be normalized and orthogonalized to each other in the ordinary way. Happily, WEM allows one to define all states and their mixing in the mathematically rigorous way, as we shall now show.

We start with the formulation in sector I and write starting from (20) the WEM equation

$$H_0\Psi_\nu(\mathbf{r}, E) + \int \frac{V_{121}(\mathbf{r}, \mathbf{r}', E)}{\eta_\nu(E)}\Psi_\nu(\mathbf{r}', E)d^3\mathbf{r}' = E\Psi_\nu(\mathbf{r}, E), \tag{55}$$

while the unperturbed states $\Psi_n(\mathbf{r})$ satisfy

$$H_0\Psi_n(\mathbf{r}) = E_n\Psi_n(\mathbf{r}). \tag{56}$$

Note that $\Psi_\nu(\mathbf{r}, E)$ depend on energy E, while $\Psi_n(\mathbf{r})$ do not. Similarly to (39), the orthogonality condition is

$$\int d\mathbf{r}d\mathbf{r}'\Psi_\nu(\mathbf{r}, E)V_{121}(\mathbf{r}, \mathbf{r}', E)\Psi_{\nu'}(\mathbf{r}', E) = -\delta_{\nu\nu'}\eta_\nu(E). \tag{57}$$

Consider now the expansion of a WEM state in the set of Ψ_n states,

$$\Psi_\nu(\mathbf{r}, E) = \sum_n c_n^\nu(E)\Psi_n(\mathbf{r}). \tag{58}$$

Taking into account that

$$\int d\mathbf{r}d\mathbf{r}'\Psi_n(\mathbf{r})V_{121}(\mathbf{r}, \mathbf{r}', E)\Psi_m(\mathbf{r}') = w_{nm}(E), \tag{59}$$

and multiplying both sides of (54) with $\Psi_{\nu'}(\mathbf{r}, E)$ and integrating over $d\mathbf{r}$, one obtains

$$\sum_n c_n^{\nu'}(E)c_n^\nu(E)(E_n - E) + \sum_{m,n}\frac{c_n^{\nu'}(E)w_{nm}(E)c_m^\nu(E)}{\eta_\nu(E)} = 0. \tag{60}$$

Thus one obtains the equation for eigenvalues $\eta_\nu(E)$

$$\det\left(\hat{E} - E + \frac{\hat{w}}{\eta_\nu(E)}\right) = 0 \tag{61}$$

which coincides with (46), obtained in sector II. Now we are specifically interested in the coefficients $\{c_n^\nu\}$, $\{c_n^{\nu'}\}$ for two different eigenvalues $\eta_\nu(E)$, $\eta_{\nu'}(E)$.

The first condition follows from (57) and (60)

$$\sum_n c_n^{\nu'}(E)c_n^{\nu}(E)(E_n - E) = \delta_{\nu\nu'}. \tag{62}$$

It is convenient to introduce reduced coefficients:

$$c_n^{\nu}(E) = \frac{\bar{c}_n^{\nu}(E)}{\sqrt{E_n - E}}; \qquad \bar{w}_{mn}(E) = \frac{w_{mn}(E)}{\sqrt{(E_m - E)(E_n - E)}}. \tag{63}$$

Then the solution for two eigenvalues in (61) is

$$\eta_\nu(E) = \frac{-((\bar{w}_{22} + \bar{w}_{11}) \pm \sqrt{(\bar{w}_{22} + \bar{w}_{11})^2 - 4\det\bar{w}})}{2}. \tag{64}$$

Here and further for notational convenience we will suppress the energy dependence of the $\bar{w}_{nm}$. The normalization condition has the form

$$\sum_n \bar{c}_n^{\nu}(E)\bar{c}_n^{\nu'}(E) = \delta_{\nu\nu'},$$
$$\sum_{n,m} \bar{c}_n^{\nu}(E)\bar{w}_{nm}(E)c_m^{\nu'}(E) = -\delta_{\nu\nu'}\eta_\nu(E). \tag{65}$$

Let us take one concrete example of two states in the subthreshold region [e.g. (2^3S_1) and (1^3D_1) states of charmonium, however at this stage they are not specified].

Keeping only two states $n = 1, 2$ e.g. for (2^3S_1) and (1^3D_1), one can write for $c_n^{\nu}(E)$, $\nu = \alpha, \beta$

$$\bar{c}_1^{\alpha}(E) = \cos\varphi(E), \qquad \bar{c}_2^{\alpha}(E) = \sin\varphi(E);$$
$$\bar{c}_1^{\beta}(E) = \sin\varphi(E), \qquad \bar{c}_2^{\beta}(E) = -\cos\varphi(E). \tag{66}$$

Note that the appearance of $O(2)$ coefficients is not accidental since $w_{nm}(E)$ is symmetric in n, m.

We are thus e.g. looking for the shifted and mixed (2^3S_1) state, denoted by α, and the same for (1^3D_1) state, denoted by β,

$$\Psi^{\alpha}(E) = \frac{\cos\varphi(E)}{\sqrt{E_1 - E}}\Psi_1 + \frac{\sin\varphi(E)}{\sqrt{E_2 - E}}\Psi_2,$$
$$\Psi^{\beta}(E) = \frac{\sin\varphi(E)}{\sqrt{E_1 - E}}\Psi_1 - \frac{\cos\varphi(E)}{\sqrt{E_2 - E}}\Psi_2. \tag{67}$$

To find $\cos\varphi(E)$, one can use the second equation in (65), which yields

$$\sin^2\varphi(E)\bar{w}_{11} - \cos\varphi(E)(\bar{w}_{12} + \bar{w}_{21}) + \cos^2\varphi(E)\bar{w}_{22} = -\eta_\beta(E),$$
$$\cos^2\varphi(E)\bar{w}_{11} - \cos\varphi(E)(\bar{w}_{12} + \bar{w}_{21}) + \sin^2\varphi(E)\bar{w}_{22} = -\eta_\alpha(E). \tag{68}$$

This gives the condition $\bar{w}_{11} + \bar{w}_{22} = -(\eta_\alpha(E) + \eta_\beta(E))$, which is identically satisfied, and the final result for $\cos^2\varphi(E)$

$$\cos^2\varphi(E) = \frac{\bar{w}_{11} - \bar{w}_{22} + D}{2D},$$
$$D = \sqrt{(\bar{w}_{11} - \bar{w}_{22})^2 + 4\bar{w}_{12}\bar{w}_{21}}. \tag{69}$$

Note that the sign of D is connected with the corresponding choice of the root in (64), for $\eta_\alpha(E)$ (lower in energy state) we have chosen the sign $+$.

It is clear that $\cos\varphi$ depends on E and therefore to define finally the mixing coefficient, one should fix the energy. For example, for the state β, the eigenvalue $\eta_\beta(E)$ crosses the line $\eta(E) = 1$ at the resonance position $E = E_\beta^R$, complex in general, and the mixing coefficient of interest from (66) is

$$c_1^{\beta} = \frac{\sin\varphi(E_\beta^R)}{\sqrt{E_1 - E_\beta^R}},$$

while the mixing coefficient of the state α is to be taken at $E = E_\alpha^R$,

$$c_2^{\alpha} = \frac{\sin\varphi(E_\alpha^R)}{\sqrt{E_2 - E_\alpha^R}}.$$

Hence, for small shifts $E_\beta^R \cong E_2$, $E_\alpha^* \approx E_1$, and energy independent φ, one recovers the symmetry condition

$$|c_1^{\beta}| \approx |c_2^{\alpha}|. \tag{70}$$

Finally, one should connect normalizations of Ψ_n and $\Psi^{\alpha,\beta}$. This can be done, if one considers the limiting case of one channel ν, where according to (59) and (57), one has

$$(c_n^{\nu}(E)w_{nm}(E)c_m^{\nu}(E)) = -\eta_\nu(E) \tag{71}$$

and for $E = E_\nu^R$ (at the resonance position), $\eta_\nu(E_\nu^R) = 1$, and for one level n from (61) one has $w_{nm}(E_\nu^R) = E_\nu^R - E_n \equiv -\Delta E_n$. Hence in the one-channel–one-level limit we have

$$(c_n^{\nu})^2\Delta E_n = 1, \qquad c_n^{\nu} = \frac{1}{\sqrt{\Delta E_n}}. \tag{72}$$

Therefore if only one level n is kept, then the normalized WEM states can be defined as

$$\bar{\Psi}^{\alpha}(E_\alpha^R) = \Psi^{\alpha}(E_\alpha^*)\sqrt{\Delta E_n}, \qquad \int(\Psi^{\alpha}(E_\alpha^R))^2 d^3r = 1, \tag{73}$$

and finally the standard normalized mixing coefficients are

$$\tilde{c}_1^{\beta} = \frac{\sin\varphi(E_\beta^R)\sqrt{\Delta E_\beta}}{\sqrt{E_1 - E_\beta^*}}, \qquad \tilde{c}_2^{\alpha} = \frac{\sin\varphi(E_\alpha^R)\sqrt{\Delta E_\alpha}}{\sqrt{E_2 - E_\alpha^*}}, \tag{74}$$

where $\Delta E_\beta = E_2 - E_\beta^R$, $\Delta E_\alpha = E_1 - E_\alpha^R$. One can see that in general coefficients are less than unity due to ratios of square roots. We finally write for $\sin\varphi$

$$\sin^2\varphi(E) = \left\{\frac{(\bar{w}_{11}-\bar{w}_{22})^2+2(\bar{w}_{12})^2+2(\bar{w}_{21})^2-(\bar{w}_{11}-\bar{w}_{22})D}{2D^2}\right\}. \quad (75)$$

Another (and physically more motivated) normalization for $\Psi^\alpha(E^*_\alpha)$ follows from (45), which can be written as

$$G^{(I)}_{Q\bar{Q}}(1,2;E) = \frac{\Psi_\alpha(1,E^R)\Psi^+_\alpha(2,E^R)}{(E^R-E)\frac{d\eta_\alpha(E^R)}{dE}}.$$

Estimating

$$\frac{dw_{nn}(E^R)}{dE} = \frac{w_{nn}(E^R)\xi}{|E^*_\alpha - E_{\rm th}|}, \qquad \xi < 1,$$

one obtains

$$\frac{d\eta_\alpha(E^*_\alpha)}{dE} = \frac{1}{E_n - E^*_\alpha} + \frac{\xi}{|E^R - E_{\rm th}|},$$

and the defacto wave functions are

$$\Psi_\alpha(1,E^R)/\sqrt{\frac{d\eta_\alpha(E^R)}{dE}},$$

which is close to (73) for $\xi \ll 1$.

VI. RESULTS AND DISCUSSION

The formalism given in this paper is based on the explicit knowledge of wave functions in both sectors I and II and yields the CC interaction operator $\hat{w}(E)$ expressed via the overlap integrals; see Eq. (8). The resulting effective interaction in each sector is energy dependent due to $\hat{w}(E)$, and violates usual orthonormality properties for wave functions. Moreover, new states appear for energies above thresholds, and one needs a rigorous formalism to treat the complete set of eigenfunctions for such operators. The WEM is indispensable for this purpose. In Eq. (46) explicit conditions are written down for Weinberg eigenvalues $\eta(E)$. It is important that $\eta(E)$ has simple analytic properties in the E plane. Therefore physical quantities expressed via $\eta(E)$, like scattering amplitude (E1) or production cross section (E2), have a definite analytic expression near the pole(s), different from the Breit-Wigner form in general. This property is more important in case of the complicated arrangement of thresholds and poles, as it is in the case of $X(3872)$; see below.

Another practical advantage of WEM is the complete set of states for each energy E, allowing one to define unambiguously symmetric mixing coefficients, as explained in Sec. V.

Before a detailed discussion of results, one should stress two main features of the closed channel pole E_n behavior under the influence of CC: (1) CC is attractive for all states below CC threshold; (2) CC is attractive in some region $E_{\rm th} \le E_n \le E^*$ above threshold and repulsive for $E > E^*$ (in the limit of small width). Both statements follow from the condition $\mathrm{Re}(w(E)) < 0$ or $\mathrm{Re}(w(E)) > 0$ in (8). As will be seen in the simplest case of one channel with lowest threshold, the 2^3P_1 pole E_n occurs in the attractive zone of the DD^* channel and hence moves down with increasing coupling.

Below we give several examples of WEM application to different problems in CC dynamics. We shall consider the following:

(i) How CC interaction changes n^3S_1 states as compared to one-channel calculations. We will calculate energy shifts and widths for the 3^3S_1 state and also mixing between 3^3S_1 and 2^3S_1 states.

(ii) We calculate eigenvalues and amplitudes in the 1^{++} state in connection with the bare 2^3P_1 level and resulting $X(3872)$ resonance.

To illustrate this formalism we will consider situations with one level in sector I and one (or many) level(s) in sector II. In Table I we present charmonium mass spectrum in the single-channel approach derived from RSH (21) (see for example [12]) in comparison with experimental data and showing the thresholds.

A. $^3S_1$ levels

As a first numerical example we consider the mass shifts and widths of the n^3S_1 ($n = 1, 2, 3$) states. For these levels the corresponding $\bar{y}^{\rm red}_{123}$ factors are

$$\bar{y}^{\rm red}_{123}(^3S_1 \to D\bar{D}) = \frac{q_i}{\sqrt{2}},$$
$$\bar{y}^{\rm red}_{123}(^3S_1 \to D^*\bar{D}) = i\epsilon_{ijm}q_m,$$
$$\bar{y}^{\rm red}_{123}(^3S_1 \to D^*\bar{D}^*) = \frac{1}{\sqrt{2}}(\delta_{ij}q_k - \delta_{jk}q_i + \delta_{ik}q_j)$$

(see Appendixes B and C) and the transition matrix element is rewritten in the following form [see Appendix C and Eq. (C2)]:

TABLE I. Charmonium spectrum in the single-channel approach derived from RSH (21) [12]. The experimental numbers are taken from the PDG [31]. All masses are in GeV.

State (thresholds)	Theory	Experiment
$1S$	3.068	3.068
$1P$	3.488	3.525
$2S$	3.678	3.674
$(D\bar{D})$		3.729
$1D$	3.787	3.771
$(D^*\bar{D})$		3.872
$2P$	3.954	3.930
$(D^*\bar{D}^*)$		4.014
$3S$	4.116	4.040

$$J_{n_1n_2n_3}(\mathbf{p}) = \frac{\gamma}{\sqrt{N_c}} \int \frac{d^3\mathbf{q}}{(2\pi)^3} \bar{y}^{\mathrm{red}}_{123}(\mathbf{p},\mathbf{q}) \Psi^{(n_1)}_{Q\bar{Q}}(c\mathbf{p}+\mathbf{q}) \times \psi^{(n_2)}_{Q\bar{q}}(\mathbf{q}) \psi^{(n_3)}_{\bar{Q}q}(\mathbf{q}), \quad (76)$$

where $\gamma \approx 1.4$ is the channel coupling parameter which is proportional to M_ω (see Appendix C) and $c = \frac{\omega_Q}{\omega_q+\omega_Q} \simeq 0.73$, where the averaged kinetic energies of heavy and light quarks in the D meson $\omega_q \simeq 0.55$ GeV, $\omega_Q \simeq 1.5$ GeV are taken from [23]. In Eq. (76), $\Psi^{(n_1)}_{Q\bar{Q}}, \ldots = R^{(n_1)}_{Q\bar{Q}}/\sqrt{4\pi}, \ldots$ are series of oscillator functions, which are fitted to realistic w.f. (see Appendix A). We obtain the latter from the solution of RSH (21) [12].

The widths and mass shifts are obtained from $|J_{n_1n_2n_3}(\mathbf{p})|^2$ averaging over initial (i) and summing over final (k, j) polarizations. Note that the final formulas for the width in channels DD, $D\bar{D}^*$, and $D^*\bar{D}^*$ differ by spin factors, which yield the ratio 1:4:7. From Eqs. (13) and (49) one can write the width taking into account relativistic corrections

$$\Gamma_{n_1n_2n_3}(\mathbf{p}) = \frac{p}{\pi} |J_{n_1n_2n_3}(\mathbf{p})|^2 \left(\frac{1}{\sqrt{\mathbf{p}^2 + M^2_{n_2}}} + \frac{1}{\sqrt{\mathbf{p}^2 + M^2_{n_3}}} \right)^{-1}, \quad (77)$$

where M_{n_2}, M_{n_3} are the masses of the corresponding D mesons. It is important that the value of the decay width strongly depends on the transition matrix element. This is illustrated by the behavior of $|J_{n_1n_2n_3}(\mathbf{p})|^2$ for the 3^3S_1 state. As can be seen from Fig. 3, $|J_{n_1n_2n_3}(\mathbf{p})|^2$ is oscillating and has two zeros, corresponding to the wave function nodes. In the small width approximation (13) the width and shift of E_n level will vanish when $p(E_n)$ approaches zero on Fig. 3. It is not a physical situation, and in the next approximation one should solve Eq. (3) in the complex plane and take into account possible mixing between states due to open channels. For instance it can be $3S$-$2S$, or $3S$-$2D$ mixing. Because of the mixing, the w.f. of the "pure" states changes and minima in Fig. 3 can be filled in by admixed states. Tables II and III give the small width values for the $3S$ state of charmonium in the $D\bar{D}$ channel, illustrating the zeros discussed above.

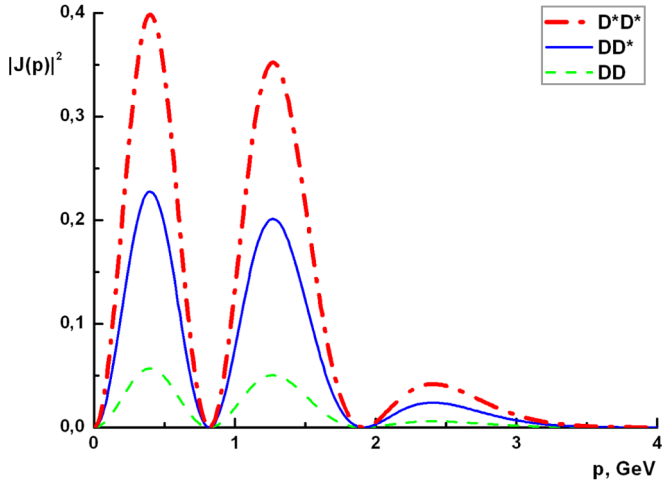

FIG. 3 (color online). The squared overlap integral $\frac{1}{3}\sum_{ijk}|J_{n_1n_2n_3}(p)|^2$ for the 3^3S_1 state.

In the WEM the shifted level positions are defined from Eq. (46) and for 3^3S_1 one obtains the picture shown in Fig. 4. The level shifts calculated from Eq. (13) are given in Table IV. One can note relatively small shifts ($\Delta E \lesssim 100$ MeV) as compared to [6,7], where $^3P_0$ and the simple harmonic oscillator (SHO) model was used, whereas in our case more complicated realistic wave functions were exploited.

In addition we have considered mixing between 3^3S_1 and 2^3S_1 levels via $D^*\bar{D}^*$ threshold, which turned out to be small, with the mixing angle [defined as in (74)] $\varphi = 5°$.

B. 2^3P_1 level

A separate discussion is needed for the s-wave decay to charmed mesons. We take as an explicit example the decay $2^3P_1 \to DD^*$. Note, that due to positive C parity the s-wave strength is mostly concentrated in the DD^* channel. In this case, the situation of Figs. 2(c) and 2(d) is realized when $\mathrm{Re}(\eta(E))$ can cross the unity line at several energy values, thus producing several resonances. In our calculations we show $\mathrm{Re}(\eta(E))$ in Fig. 5 which correspond to different values of channel coupling parameter in the region $\pm 30\%$ around the standard value $\gamma = 1.4$ ($M_\omega = 0.8$ GeV). As can be seen, $\mathrm{Re}(\eta(E))$ intercepts the line $\mathrm{Re}(\eta(E)) = 1$ 3 times. However we have to take into account imaginary parts above the thresholds. The simplest way is to calculate factor $|\eta(E)|^2/|1-\eta(E)|^2$ which appears in the squared t matrix (40). The result is the two-resonance structure, one of which is near threshold $M \sim 3.872$ GeV and another one near $M \sim 3.940$ GeV; the latter becomes increasingly broad with increasing coupling γ to open channel. In the recent work [33] a similar form of the first peak was suggested. We note that the factor $|\eta(E)|^2/|1-\eta(E)|^2$ is relevant for the t matrix of DD^* scattering, while new charmonium resonances were observed in production cross sections like $e^+e^- \to DD^*$ or $B \to K(DD^*)$. Therefore we define the production yield

TABLE II. The decay width $\Gamma_{n_1n_2n_3}(\mathbf{p})$ of 3^3S_1 charmonium state. The resonance momentum p is taken from the PDG [31].

Channel	p, GeV	$\Gamma(p)$, MeV
$D\bar{D}$	0.777	0.31
$D^*\bar{D}$	0.576	25.5
$D^*\bar{D}^*$	0.227	17.8

TABLE III. Ratios of branching fractions for 3^3S_1 state.

Ratio	Experiment [32]	This paper	$^3P_0$ [17]
$\mathcal{B}(\psi(4040) \to D\bar{D})/\mathcal{B}(\psi(4040) \to D^*\bar{D})$	0.24 ± 0.17	0.012	0.003
$\mathcal{B}(\psi(4040) \to D^*\bar{D}^*)/\mathcal{B}(\psi(4040) \to D^*\bar{D})$	0.18 ± 0.18	0.70	1.0

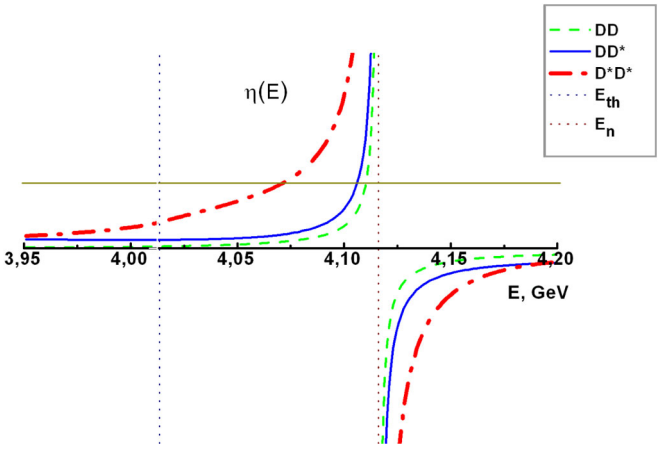

FIG. 4 (color online). The Weinberg eigenvalue $\mathrm{Re}(\eta(E))$ for the 3^3S_1 state, where $E_n = 4.116$ GeV is the eigenvalue of the single-channel relativistic string Hamiltonian H_0 (bare resonance) and $E_{\mathrm{th}}(D^*\bar{D}^*) = 4.014$ GeV denotes the closest threshold.

TABLE IV. Mass shifts (in MeV) of the n^3S_1 states with $n = 1, 2, 3$.

State	DD	$D\bar{D}^*$	$D^*\bar{D}^*$	Total
1^3S_1	−5	−19	−30	−54
2^3S_1	−15	−41	−56	−112
3^3S_1	−6	−10	−45	−61

$|A_3(E)|^2$, given in (E2) and show in Fig. 6 the quantity

$$\frac{\mathrm{Im}w_{nn}(E)}{|E - E_n - w_{nn}(E)|^2} \sim \frac{\mathrm{Im}\eta(E)}{|1 - \eta(E)|^2(E - E_n)}.$$

In our approximation ($D_0D_0^*$ and $D_+D_-^*$ thresholds coincide and there is no connection to $\omega J/\psi$ and $J/\psi\pi\pi$ channels), one can see the double peak structure for $\gamma = 1.0$; the first peak at 3.872 GeV is accompanied by a wide peak around 3.940 GeV. However, with increasing γ, when $\gamma = 1, 2$, the peak in Fig. 6 at 3940 becomes flat, while the lower peak at 3.872 GeV is narrow and high. This picture corresponds to the experimental situation.

The case when both thresholds $D_0D_0^*$ and $D_+D_-^*$ are taken into account is illustrated by Fig. 5 for $\mathrm{Re}(\eta(E))$ and Fig. 7 for the production cross section. As can be seen, the curves for the production cross section depend strongly on channel coupling parameter γ. For $\gamma = 1.0$ [line (2)] which is 30% smaller than the nominal value $\gamma = 1.4$ ($M_\omega = 0.8$ GeV) one can see a peak at the higher threshold $D_+D_-^*$ and a wider peak at 3.940 GeV; however for $\gamma = 1.2$ [line (4)], the 3.940 GeV peak flattens and simultaneously the peak appears at the lower threshold $D_0D_0^*$, while only a week cusp is seen at the higher threshold $D_+D_-^*$. Surprisingly, the isotopically equivalent thresholds (which we take into account with equal weight), due to different position in the energy plane, provide finally the asymmetric picture observed in experiment [22].

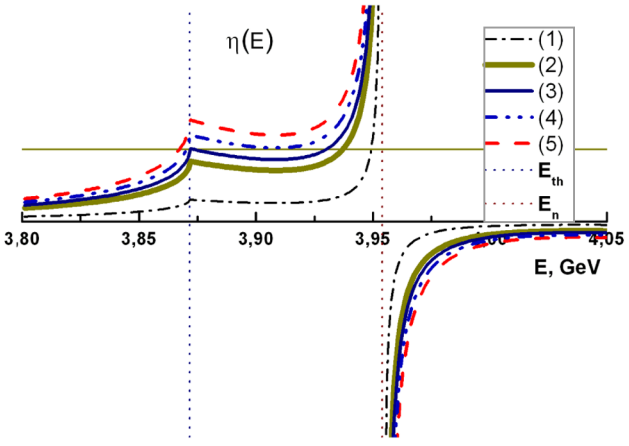

(a) One threshold, $E_{th}(D_0D_0^*)$=3.872 GeV.

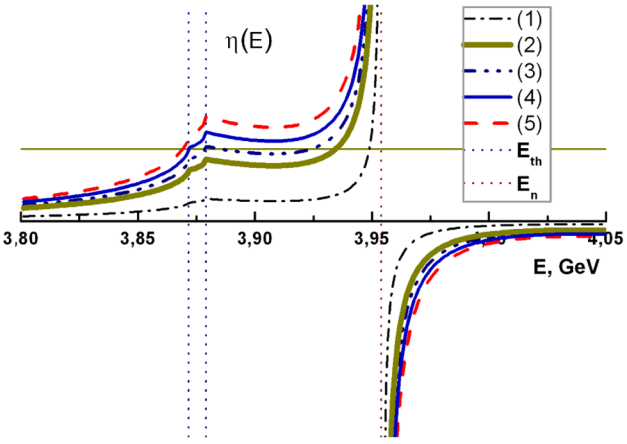

(b) Two thresholds, $E_{th}(D_0D_0^*; D_+D_-^*)$=3.872; 3.879 GeV.

FIG. 5 (color online). The Weinberg eigenvalue $\mathrm{Re}(\eta(E))$ for the 2^3P_1 state with different values of channel coupling parameter [(1)—$\gamma = 0.6$, (2)—$\gamma = 1.0$, (3)—$\gamma = 1.1$, (4)—$\gamma = 1.2$, (5)—$\gamma = 1.3$], $E_n = 3.954$ GeV is the eigenvalue of the single-channel relativistic string Hamiltonian H_0 (bare resonance) and $E_{\mathrm{th}}(D_0D_0^*; D_+D_-^*) = 3.872$; 3.879 GeV denote thresholds.

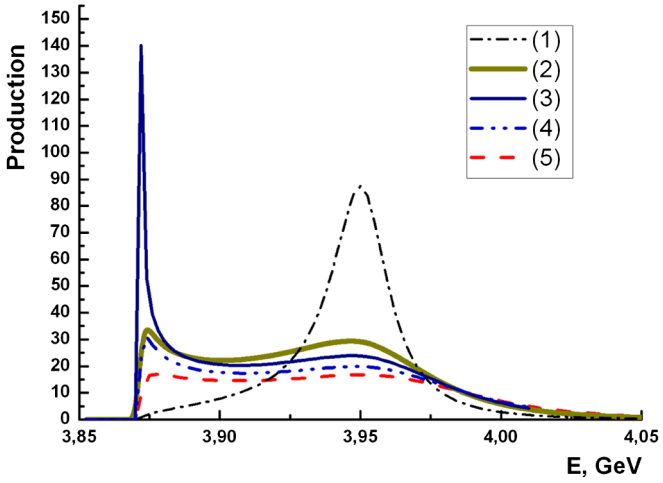

FIG. 6 (color online). Production cross section $\sim \frac{\mathrm{Im}w_{nn}(E)}{|E-E_n-w_{nn}(E)|^2}$ for the 1^{++} state with different values of channel coupling parameter [(1)—$\gamma = 0.6$, (2)—$\gamma = 1.0$, (3)—$\gamma = 1.1$, (4)—$\gamma = 1.2$, (5)—$\gamma = 1.3$]. For small values of channel coupling parameter γ [line (1)] one can see a good Breit-Wigner shape, which corresponds to the shifted 2^3P_1 state, while for larger γ [lines (2), (3), (4)] there is a broadening of higher resonance together with a steep rise near the threshold $E_{\mathrm{th}}(D\bar{D}^*) = 3.872$ GeV.

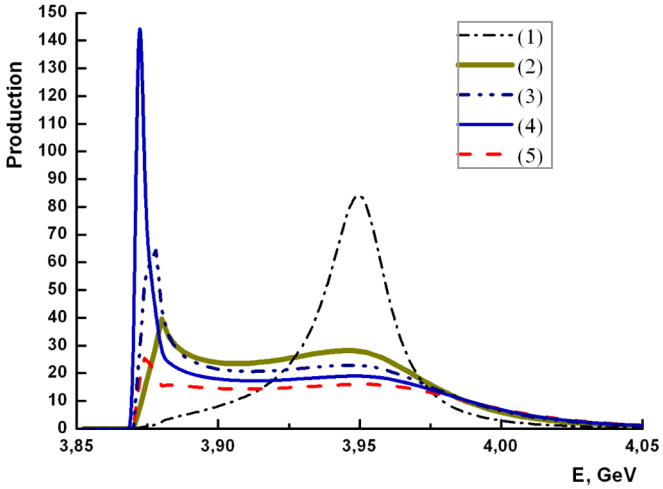

FIG. 7 (color online). Production cross section $\sim \frac{\mathrm{Im}w_{nn}(E)}{|E-E_n-w_{nn}(E)|^2}$ for the 1^{++} state with different values of channel coupling parameter [(1)—$\gamma = 0.6$, (2)—$\gamma = 1.0$, (3)—$\gamma = 1.1$, (4)—$\gamma = 1.2$, (5)—$\gamma = 1.3$] in the case, when both thresholds $D_0D_0^*$ and $D_+D_-^*$ are taken into account separately. For small values of channel coupling parameter γ [line (1)] one can see a good Breit-Wigner shape, which corresponds to the shifted 2^3P_1 state, while for larger γ [line (2)] there is a broadening together with a cusp first near the closest threshold $E_{\mathrm{th}}(D_+D_-^*) = 3.879$ GeV and then for $\gamma = 1.2$ [line (4)] a sharp peak appears at the $E_{\mathrm{th}}(D_0D_0^*) = 3.872$ GeV.

VII. SUMMARY

We have formulated equations for Green's functions of strongly coupled sectors, where new resonances can appear due to CC interaction. We found that the best formalism for the CC induced energy-dependent interaction is the Weinberg eigenvalue method. Conditions for the poles and their positions were systematically studied in the cases of P-wave and S-wave channel coupling. In the first case one finds only displacement of poles, while in the second new resonances appear, and in the $^3P_1$ case two peaks at 3.872 and 3.940 GeV were found with the height depending on the coupling constant M_ω. Moreover, we have shown in Fig. 7 that at one value of M_ω the lower peak is at the $D_0D_0^*$ threshold (but not at the $D_+D_-^*$ threshold) and at the same time the upper peak at 3.940 GeV flattens. This situation corresponds to the experimental data [22] and supports our dynamical CC mechanism.

Mixing of n^3S_1 states was formulated in WEM and found to be small, while shifts of 3^3S_1 are of the order 50–80 MeV, which signals necessity of mass renormalization.

The method developed in the present paper provides a rigorous definition of resonance wave functions and mixings in the case of strongly coupled channels.

ACKNOWLEDGMENTS

The authors are grateful to Yu. S. Kalashnikova for numerous discussions, suggestions, and help, to A. M. Badalian for useful discussions and remarks, to A. I. Veselov for suggestions and help with computer programs, and to A. E. Kudryavtsev for good questions. The financial help of the *Dynasty Foundation* to I. V. D. and RFFI Grant No. 09-02-00629a and Grant No. NS-4961.2008.2 are gratefully acknowledged.

APPENDIX A: WAVE FUNCTIONS

In Eq. (76) $R^{(n_1)}_{Q\bar{Q}}$, $R^{(n_2)}_{Q\bar{q}}$, and $R^{(n_3)}_{\bar{Q}q}$ are series of oscillator wave functions, which are fitted to realistic wave functions. We obtain them from the solution of the relativistic string Hamiltonian (21), described in [9,12,25].

In position space the basic SHO radial wave function is given by

$$R^{\mathrm{SHO}}_{nl}(\beta, r) = \beta^{3/2}\sqrt{\frac{2(n-1)!}{\Gamma(n+l+1/2)}} \times (\beta r)^l e^{-\beta^2 r^2/2} L^{l+1/2}_{n-1}(\beta^2 r^2),$$

$$\int_0^\infty (R^{\mathrm{SHO}}_{nl}(\beta, r))^2 r^2 dr = 1, \tag{A1}$$

where β is the SHO wave function parameter, and $L^{l+1/2}_{n-1}(\beta^2 r^2)$ is an associated Laguerre polynomial. The realistic radial wave function can be represented as an expansion in the full set of oscillator radial functions:

TABLE V. Effective values β (in GeV) and coefficients c_k of the series of oscillator radial wave functions $R_{kl}^{\rm SHO}(\beta, r)$ which are fitted to realistic radial wave functions $R_{nl}(r)$ of charmonium and D meson.

State	β	Coefficients c_k				
			Charmonium			
$1S$	0.70	$c_1 = 0.977\,96$	$c_2 = 0.169\,169$	$c_3 = 0.117\,682$	$c_4 = 0.019\,694$	$c_5 = 0.025\,113$
$2S$	0.53	$c_1 = -0.118\,89$	$c_2 = -0.972\,774$	$c_3 = -0.134\,041$	$c_4 = -0.142\,303$	$c_5 = 0.000\,142$
$3S$	0.46	$c_1 = -0.093\,54$	$c_2 = 0.149\,573$	$c_3 = 0.958\,816$	$c_4 = 0.112\,102$	$c_5 = 0.183\,886$
$2P$	0.48	$c_1 = -0.062\,71$	$c_2 = 0.981\,834$	$c_3 = -0.123\,392$	$c_4 = 0.127\,111$	$c_5 = 0.000\,495$
			D meson			
$1S$	0.48			$c = 1$		

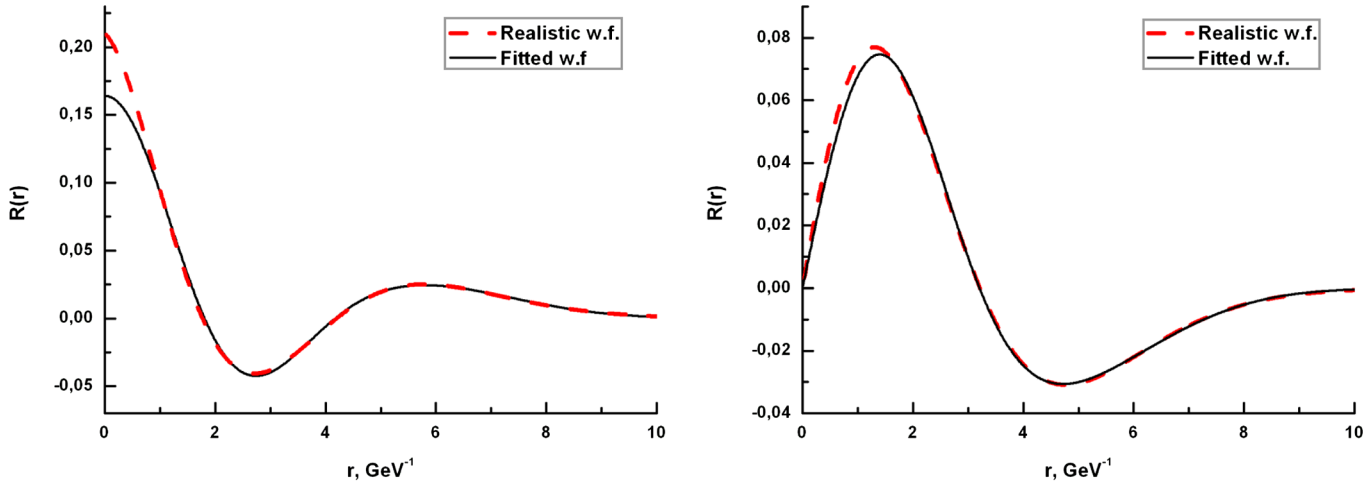

(a) $R^{(n_1)}_{Q\bar{Q}}(3S)/\sqrt{4\pi}$ (b) $R^{(n_1)}_{Q\bar{Q}}(2P)/\sqrt{4\pi}$

FIG. 8 (color online). Realistic radial w.f. (divided by $\sqrt{4\pi}$) of charmonium $3S$ and $2P$ states (broken lines) and the series of oscillator functions with $k_{\rm max} = 5$ (solid lines). Note that the solid curves are almost indistinguishable from the broken ones.

$$R_{nl}(r) = \sum_{k=1}^{k_{\rm max}} c_k R_{kl}^{\rm SHO}(\beta, r). \tag{A2}$$

Effective values of oscillator parameters β and coefficients c_k are obtained minimizing χ^2 and listed in Table V. The quality of approximations can be seen from Fig. 8. In the momentum space the SHO radial wave function is given by

$$R_{nl}^{\rm SHO}(\beta, p) = \frac{(-1)^n (2\pi)^{3/2}}{\beta^{3/2}} \times \sqrt{\frac{2(n-1)!}{\Gamma(n+l+1/2)}} \left(\frac{p}{\beta}\right)^l e^{-p^2/2\beta^2} L_{n-1}^{l+1/2}\left(\frac{p^2}{\beta^2}\right),$$

$$\int_0^\infty (R_{nl}^{\rm SHO}(\beta, p))^2 \frac{p^2 dp}{(2\pi)^3} = 1.$$

APPENDIX B: THE VERTEX OPERATORS AND SPINOR EXPRESSIONS IN THE (2×2) FORM

Our purpose here is to go from Eq. (8), where $\bar{y}_{123}$ is the trace of (4×4) form to the (2×2) or spinor form, defining in this way $\bar{y}^{\rm red}_{123}$.

We consider operators of the form $(\bar{\psi}\Gamma_i\psi)$, with Γ_i consisting of Dirac matrices γ_i and derivatives $\overleftrightarrow{\partial}_i$. To proceed to the (2×2) form, one exploits the limit $M \to \infty$ of the heavy quark mass, so that for the light quark in the heavy-light meson the Dirac equation can be used, and one can use the symbolically Dirac one-body equation, $(\boldsymbol{\alpha}\mathbf{p} + \beta(m + U))\psi = (\varepsilon - V)\psi$, so that for $\psi = \binom{v}{w}$, one has $w = \frac{1}{m+U-V+\varepsilon}(\boldsymbol{\sigma}\mathbf{p})v$. One can also use connection $\bar{\psi} = C^{-1}\psi^c = \psi^c(C^{-1})^T$, where $C = (C^{-1})^T = \gamma_2\gamma_4$, $\gamma_i = -i\beta\alpha_i$, so that $\bar{\psi}\Gamma_i\psi = (v^c, w^c)\gamma_2\gamma_4\Gamma_i\binom{v}{w}$. Note that spin indices of charge-conjugated spinors are connected to ordinary spinors by matrix σ_2: $v^c\sigma_2 = -(\sigma_2 v^c)^T \equiv \tilde{v}^c$, and for w^c one has

$$w^c\sigma_2 = \left(\frac{1}{m + U - V + \varepsilon}\boldsymbol{\sigma}\mathbf{p}v^c\right)^T\sigma_2 = -\tilde{v}^c\boldsymbol{\sigma}\overleftarrow{\mathbf{p}}\frac{1}{m + U - V + \varepsilon} \equiv -\tilde{w}^c, \tag{B1}$$

where the notation $\overleftarrow{\mathbf{p}}$ implies that the operator acts on the left. We are considering the 7 lowest states and display in Table VI the operator Γ_i, the corresponding quantum num-

TABLE VI. Bilinear operators $\bar{\psi}\Gamma_i\psi$ and their (2×2) forms (see the notations in the text).

J^{PC}	$2S+1L_J$	Γ_i	(2×2) form
0^{-+}	$^1S_0$	$-i\gamma_5$	$\tilde{v}^c v - \tilde{w}^c w$
1^{--}	$^3S_1$	γ_i	$-(\tilde{v}^c\sigma_i v + \tilde{w}^c\sigma_i w)$
1^{+-}	$^1P_1$	$-i\gamma_5\overleftrightarrow{\partial}_i$	$\tilde{v}^c\overleftrightarrow{\partial}_i v - \tilde{w}^c\overleftrightarrow{\partial}_i w$
0^{++}	$^3P_0$	1	$i(\tilde{v}^c w - \tilde{w}^c v)$
1^{++}	$^3P_1$	$\gamma_i\gamma_5$	$-(\tilde{v}^c\sigma_i w + \tilde{w}^c\sigma_i v)$
2^{++}	$^3P_2$	$\gamma_i\overleftrightarrow{\partial}_k + \gamma_k\overleftrightarrow{\partial}_i - \frac{2}{3}\delta_{ik}\hat{\partial}$	$-(\tilde{v}^c\rho_{ik} v + \tilde{w}^c\rho_{ik} w)$
2^{-+}	$^1D_2$	$(\overleftrightarrow{\partial}_i\overleftrightarrow{\partial}_k - \frac{1}{3}\delta_{ik}(\overleftrightarrow{\partial})^2)\gamma_5$	$i(\tilde{v}^c\omega_{ik} w - \tilde{w}^c\omega_{ik} v)$
2^{--}	$^3D_2$	$(\gamma_i\overleftrightarrow{\partial}_k + \gamma_k\overleftrightarrow{\partial}_i - \frac{2}{3}\delta_{ik}\hat{\partial})\gamma_5$	$-(\tilde{v}^c\rho_{ik} w + \tilde{w}^c\rho_{ik} v)$
1^{--}	$^3D_1$	$\gamma_i\omega_{ik}$	$-(v^c\sigma_i\omega_{ik} v + \tilde{w}^c\sigma_i\omega_{ik} w)$

bers J^{PC}, spectroscopic notation $^{2S+1}L_J$, and the equivalent (2×2) form for the same vertex Γ_i in the last column. We are using in Table VI the following notations:

$$\rho_{ik} \equiv \sigma_i\overleftrightarrow{\partial}_k + \sigma_k\overleftrightarrow{\partial}_i - \tfrac{2}{3}\sigma_l\overleftrightarrow{\partial}_i\delta_{ik};$$
$$\omega_{ik} \equiv \overleftrightarrow{\partial}_i\overleftrightarrow{\partial}_k - \tfrac{1}{3}\delta_{ik}(\overleftrightarrow{\partial})^2, \qquad \hat{\partial} \equiv \overleftrightarrow{\partial}_i\gamma_i.$$

Note that in the 2×2 form one has

$$^3P_0\text{: } \tilde{v}^c\frac{\boldsymbol{\sigma}\overleftrightarrow{\mathbf{p}}}{m+U-V+\varepsilon}v,$$
$$^3P_1\text{: } -ie_{ikl}\tilde{v}^c\frac{\overleftrightarrow{p}_k\sigma_l}{m+U-V+\varepsilon}v,$$
$$^1D_2\text{: } \tilde{v}^c\frac{\boldsymbol{\sigma}\overleftrightarrow{\mathbf{p}}}{m+U-V+\varepsilon}\omega_{ik}v.$$

In the (2×2) form one can write a wave function of charmonium and D mesons $(\Psi^{(n_1)}_{Q\bar{Q}}, \psi^{(n_2)}_{Q\bar{q}}, \psi^{(n_3)}_{\bar{Q}q})$ as $\Psi_{\text{meson}} = \text{const}\varphi_{nl}(r)(\tilde{v}^c\Gamma^{(n)}_{\text{red}}v)$ and normalize it as

$$\|\Psi_{\text{meson}}\|^2 = 1 = \int|\varphi_{nl}(r)|^2r^2dr\,\text{tr}\{\Gamma^{(n)}_{\text{red}}\Gamma^{(n)+}_{\text{red}}\}d\Omega. \quad \text{(B2)}$$

Defining $\varphi_{nl}(r) = R_{nl}(r)/\sqrt{4\pi}$, the normalization condition for the angular part takes the form $\int\text{tr}\{\Gamma^{(n)}_{\text{red}}\Gamma^{(n)+}_{\text{red}}\}\times\frac{d\Omega}{4\pi} = 1$. Then $J_{n_1n_2n_3}(\mathbf{p})$ can be written as in (7), but $\bar{y}^{\text{red}}_{123}$ can be found in spinor (2×2) form as

$$\bar{y}^{\text{red}}_{123} = \text{tr}\{\Gamma^{(n_1)}_{\text{red}}\Gamma^{(n_2)}_{\text{red}}(\boldsymbol{\sigma}\mathbf{q})\Gamma^{(n_3)}_{\text{red}}\}, \quad \text{(B3)}$$

see Table VII, and all $\Gamma^{(n)}_{\text{red}}$ are normalized as written above. Hence e.g.

$$\Gamma^{(n_{2,3})}_{\text{red}}(D) = \frac{1}{\sqrt{2}}, \qquad \Gamma^{(n_{2,3})}_{\text{red}}(D^*) = \frac{\sigma_i}{\sqrt{2}}.$$

APPENDIX C: THE PAIR-CREATION VERTEX

In the same way we consider here the (2×2) reduction of the pair-creation vertex, taking ψ, $\bar{\psi}$ for light quarks as solutions of the Dirac equation and writing the effective string-breaking Lagrangian as

$$\mathcal{L}_{sb} = \int\bar{\psi}(u)M_\omega\psi(u)d^4u$$
$$= M_\omega\int\frac{i\tilde{v}_c\boldsymbol{\sigma}\overleftrightarrow{p}v}{m+U-V+\varepsilon_0}d^4u \quad \text{(C1)}$$

and we have denoted $U \equiv \sigma r$; $V \equiv -\frac{4}{3}\frac{\alpha_s}{r}$; $\overleftrightarrow{p} = \mathbf{p} - \overleftarrow{p}$; ε_0 is the Dirac eigenvalue $\varepsilon_0 = M_0(\bar{Q}q) - M_{\bar{Q}}$, $\tilde{v}_c = v_c\sigma_2$ is the spinor of antiquark, and M_ω is the same as in Eq. (3).

One can take in (C1) the averaged value of the denominator $\langle m+U-V+\varepsilon_0\rangle \to m+\langle U\rangle - \langle V\rangle + \varepsilon_0$ which effectively redefines our vertex constant M_ω. As a result

TABLE VII. The $\Gamma^{(n_1)}_{\text{red}}$ operator and nonrelativistic form $\bar{y}^{\text{red}}_{123}$ for $D\bar{D}$, $D\bar{D}^*$, and $D^*\bar{D}^*$ channels.

J^{PC}	$^{2S+1}L_J$	$\Gamma^{(n_1)}_{\text{red}}$	$\bar{y}^{\text{red}}_{123}$		
			$D\bar{D}$	$\frac{1}{\sqrt{2}}(D\bar{D}^* \pm \bar{D}D^*)$	$D^*\bar{D}^*$
0^{-+}	$^1S_0$	$\frac{1}{\sqrt{2}}$	$\cdots$	q_j	$\frac{i}{\sqrt{2}}\epsilon_{jmk}q_m$
1^{--}	$^3S_1$	$\frac{1}{\sqrt{2}}\sigma_i$	$\frac{1}{\sqrt{2}}q_i$	$i\epsilon_{ijm}q_m$	$\frac{1}{\sqrt{2}}(\delta_{ij}q_k - \delta_{jk}q_i + \delta_{ik}q_j)$
1^{+-}	$^1P_1$	$\sqrt{\frac{3}{2}}n_i$	$\cdots$	$\sqrt{3}n_iq_j$	$i\sqrt{\frac{3}{2}}\epsilon_{jmk}q_mn_i$
0^{++}	$^3P_0$	$\frac{1}{\sqrt{2}}\boldsymbol{\sigma}\mathbf{n}$	$\frac{1}{\sqrt{2}}(\mathbf{qn})$	$\cdots$	$\frac{1}{\sqrt{2}}(q_kn_j + q_jn_k - \delta_{jk}(\mathbf{qn}))$
1^{++}	$^3P_1$	$\frac{\sqrt{3}}{2}\epsilon_{ikl}\sigma_kn_l$	$\cdots$	$i\sqrt{\frac{3}{2}}(q_in_j - (\mathbf{qn})\delta_{ij})$	$\cdots$
2^{++}	$^3P_2$	$\frac{3}{4}(\sigma_in_l + \sigma_ln_i - \frac{2}{3}(\boldsymbol{\sigma}\mathbf{n})\delta_{il})$	$\cdots$	$\cdots$	$\frac{3}{4}(n_l(q_k\delta_{ij} - q_i\delta_{jk} + q_j\delta_{ik}) + n_i(q_k\delta_{lj} - q_l\delta_{jk} + q_j\delta_{lk})$ $-n_j(\frac{2}{3}q_k\delta_{il}) - n_k(\frac{2}{3}q_j\delta_{il}) + \frac{2}{3}(\mathbf{qn})\delta_{il}\delta_{j,k})$

the reduced form of the matrix element $J(p)$ in Eq. (8) assumes the form

$$J(\mathbf{p}) = \frac{\gamma}{\sqrt{N_c}} \int \frac{d^3q}{(2\pi)^3} \bar{y}^{\rm red}_{123}(\mathbf{p},\mathbf{q}) \Psi^{+(n_1)}_{Q\bar{Q}}(c\mathbf{p}+\mathbf{q}) \times \Psi^{(n_2)}_{Q\bar{q}}(\mathbf{q}) \Psi^{(n_3)}_{\bar{Q}q}(\mathbf{q}), \tag{C2}$$

where $\bar{y}^{\rm red}_{123}$ is given in Table VII and $\gamma \equiv \frac{2M_\omega}{m+\langle U\rangle-\langle V\rangle+\varepsilon_0}$. One can find values of $\langle U\rangle$, $\langle V\rangle$, and ε_0 in Table VIII, and persuade oneself that γ is rather stable for different α_s and numerically $\gamma = \frac{2\cdot 0.8\ \rm GeV}{1.2\ \rm GeV} \approx 1.4$.

To check consistency of our approximation of putting average values into the denominator, we have compared normlization conditions of bispinors $(v^+v)+(w^+w) = 1 = v^+(1+\frac{\mathbf{p}^2}{(\varepsilon+\langle U\rangle-\langle V\rangle+m)^2})v$, and found that the term with the denominator contributes around 20%, and we expect the same accuracy in the definition of γ. Actually, we are always varying γ in the region $\pm 30\%$ around the nominal value $\gamma = 1.4$.

One can also check at this point how the (4×4) vertex $M_\omega \bar{y}_{123}$ goes over into the reduced form $\gamma\bar{y}^{\rm red}_{123}$. For example, for the 1^{--} state decaying into DD^* one has in the heavy quark mass limit (see e.g. [13,14]). $\bar{y}_{123} = \frac{iq_n e_{ikn}}{\omega_q}$, and $\omega_q \approx 0.6$ GeV is the average energy of the light quark, which coincides with $1/2$ of the denominator in γ, while $\bar{y}^{\rm red}_{123}$ from Table VII is $iq_n e_{ikn}$. Thus indeed one has equality $M_\omega \bar{y}_{123} = \gamma \bar{y}^{\rm red}_{123}$.

For practical reasons we have used for our calculations the reduced (2×2) forms everywhere.

In the nonrelativistic limit one has

$$\mathcal{L}_{sb} = iM_\omega \int \tilde{v}_c \frac{\sigma \overleftrightarrow{p}}{2m} v d^4u \tag{C3}$$

and for the plane-wave (free) quarks, $v = e^{i\mathbf{k}\mathbf{u}}u(\alpha)/\sqrt{2\varepsilon_0 V_3}$, one has $\tilde{v}_c = \tilde{u}_c e^{-i\mathbf{k}\mathbf{u}}/\sqrt{2\varepsilon_0 V_3}$

$$\mathcal{L}_{sb} = i\frac{(\tilde{u}_c \boldsymbol{\sigma} \overleftrightarrow{p} u)}{4m}. \tag{C4}$$

TABLE VIII. Dirac eigenvalues ε_0 (in GeV) for quarks of different masses m (in GeV) and α_s. The averaged potentials $\langle U\rangle$, $\langle V\rangle$ (in GeV) for different α_s are also presented.

α_s	0	0.3	0.39
$m = 0.005$	0.65	0.493	0.424
$m = 0.15$	0.80	0.584	0.509
$m = 0.2$	0.838	0.617	0.539
$\langle U\rangle$	0.573	0.486	0.463
$\langle V\rangle$	0	−0.198	−0.273

APPENDIX D: DERIVATION OF EQ. (40), ETC.

To introduce the Weinberg method it is useful to start from the well-known Hilbert-Schmidt method in integral equations with symmetric kernels $K(x,y)$, where x, y belong to the n-dimension space. The eigenvalue equation has the form

$$\phi_n(x) = l_n \int K(x,y)\phi_n(y)dy. \tag{D1}$$

The spectral decomposition and the resolvent are

$$K(x,y) = \sum \frac{\phi_n(x)\phi_n(y)}{l_n} \Gamma(x,y;l) = \sum \frac{\phi_n(x)\phi_n(y)}{(l_n - l)} \tag{D2}$$

and the orthonormality conditions:

$$\int \phi_n \phi_m dx = \delta_{mn}, \tag{D3}$$

$$\int \phi_n K(x,y)\phi_m dxdy = \frac{1}{l_n}\delta_{mn}. \tag{D4}$$

In the case discussed in Sec. IV, one arrives at Eqs. (37)–(40), starting from equation

$$\Psi = -\frac{1}{H_0 - E}\hat{V}\Psi \tag{D5}$$

and performs symmetrization, using definitions $\phi_n = \sqrt{H_0 - E}\Psi_\nu$,

$$K = -\frac{1}{\sqrt{H_0 - E}}\hat{V}\frac{1}{\sqrt{H_0 - E}}, \qquad l_n = \frac{1}{\eta_\nu}. \tag{D6}$$

Now Eq. (D3) yields (42), where a_ν is defined in (41), Eq. (D4) gives (39). Similarly, the Green's function is connected to the resolvent

$$G = \frac{1}{H_0 - E + V} = \frac{1}{\sqrt{H_0 - E}}(1+\Gamma)\frac{1}{\sqrt{H_0 - E}} = \sum_\nu \Psi_\nu \frac{1}{(1-\eta_\nu)}\Psi_\nu. \tag{D7}$$

Now we turn to the t matrix. One has

$$t = \hat{V} - \hat{V}G\hat{V}; \qquad H = H_0 + \hat{V}, \tag{D8}$$

where $\hat{V} = V_{121}$ in sector I. One can rewrite (D8)

$$t = H_0 - E + \sum_\nu (H_0 - E)\Psi_\nu \frac{1}{\eta_\nu - 1}\Psi_\nu (H_0 - E) = H_0 - E + \sum_\nu \frac{a_\nu(p,E)a_\nu(p',E)}{\eta_\nu - 1} = H_0 - E - \sum_\nu \frac{\eta_\nu a_\nu a_\nu}{1-\eta_\nu} - \sum_\nu a_\nu a_\nu. \tag{D9}$$

For the latter sum one writes

$$\sum_\nu a_\nu a_\nu = \sum_{\nu,n,n'} c_{\nu n}(E_n - E)\Psi_n(p) c_{\nu n'}(E_{n'} - E)\Psi_{n'}(p')$$
$$= \sum_{\nu n n'} (E_n - E)\bar{c}^\nu_n \bar{c}^\nu_{n'} \Psi_n \Psi_{n'}$$
$$= \sum_n (E_n - E)\Psi_n \Psi_n = \langle p|(H_0 - E)|p'\rangle, \quad \text{(D10)}$$

where (65) was used. Hence finally one gets Eq. (36)

$$t = -\sum_\nu \frac{\eta_\nu a_\nu(p,E) a_\nu(p',E)}{1-\eta_\nu(E)}. \quad \text{(D11)}$$

APPENDIX E: ANALYTIC STRUCTURE OF WEINBERG AMPLITUDES AND POLE POSITIONS

In this Appenix we study the analytic structure of production and scattering amplitudes induced by CC resonances. We consider two types of amplitudes, the scattering amplitude in sector II, e.g. $A(D\bar{D}^* \to D\bar{D}^*)$, and production amplitude of the type $(Q\bar{Q}) \to (Q\bar{q})(\bar{Q}q)$, which appears in processes e.g. $e^+e^- \to D\bar{D}^*, \ldots$ or $B \to K(Q\bar{Q}) \to K(D\bar{D}^*)$.

In the first case the relevant part of the amplitude is given in (40), and can be written as

$$A_1(E) = \frac{\eta_\nu(E)}{1-\eta_\nu(E)}, \quad \text{or} \quad A_2(E) = \frac{1-\eta^*_\nu(E^\nu)}{1-\eta_\nu(E)}. \quad \text{(E1)}$$

In the second case one can start from (D7) for $(Q\bar{Q})$ Green's function and persuade oneself that neglecting mixing of states one returns to the expression (10). The production cross section is proportional to the imaginary part of $G_{Q\bar{Q}}$ on the cut, starting from the threshold of interest (e.g. $D\bar{D}^*$) and can be written as

$$|A_3(E)|^2 = \frac{1}{2i}\Delta G^{(I)}_{Q\bar{Q}}$$
$$= \sum_n \Psi^{(n)}_{Q\bar{Q}}(1) \frac{-\mathrm{Im}(w_{nn}(E))}{|E - E_n - w_{nn}(E)|^2} \Psi^{(n)}_{Q\bar{Q}}(2). \quad \text{(E2)}$$

One can easily find that the latter expression is proportional to $\Psi_\nu(1)\frac{\mathrm{Im}\,\eta_\nu(E)}{|1-\eta_\nu(E)|^2}\Psi_\nu(2)$, so that of crucial importance is the analytic structure of $\frac{1}{1-\eta_\nu(E)}$.

We consider the case , when only one bare $Q\bar{Q}$ state E_n is retained, assuming that other states are far off and mixing of states, discussed in Sec. V is unimportant as compared to the direct influence of the decay channel. In this case one can write

$$\eta_\nu(E) = \frac{w_{nn}(E)}{E - E_n} \quad \text{(E3)}$$

and we write $w_{nn}(E) \equiv w(E)$

We write $w(E)$ as

$$w(E) = \int \frac{d^3\mathbf{p}}{(2\pi)^3} \frac{(J(\mathbf{p}))^2}{E - E(\mathbf{p})} = \frac{\bar{c}}{2}\int_0^\infty \frac{\sqrt{u}duf(u)}{z-u}, \quad \text{(E4)}$$

where $\bar{c} = \frac{\tilde{M}}{\pi^2}$, $E(\mathbf{p}) = E_{\mathrm{th}} + \frac{\mathbf{p}^2}{2\tilde{M}}$, $z = 2\tilde{M}(E - E_{\mathrm{th}})$ and finally

$$f(u) = f(\mathbf{p}^2) = (J(\mathbf{p}))^2. \quad \text{(E5)}$$

Since $f(\mathbf{p}^2) > 0$ for all real $\mathbf{p}^2$, one has

$$w(0) = -\frac{\bar{c}}{2}\int_0^\infty \frac{du}{\sqrt{u}} f(u) < 0. \quad \text{(E6)}$$

It is convenient to continue $f(u)$ analytically in the region near the real axis[4] and rewrite (E4) as a contour integral along the contour C circumjacent to the cut in the u plane

$$w(z) = \frac{\bar{c}}{4}\int_C \frac{\sqrt{u}duf(u)}{z-u}.$$

It is clear that the same integral along the contour C' with the point z inside C^1 does not have singularities on the first sheet, hence one can represent $w(z)$ as follows (the difference of two integrals is the residue at the pole $u = z$)

$$w(z) = -\frac{i\pi}{2}\bar{c}\sqrt{z}f(z) + F(z), \quad \text{(E7)}$$

where $F(z)$ is a nonsingular function which can be Taylor expanded around $z = 0$.

In (E7) the argument of z is chosen in a standard way: $\arg(z) = 0$, for $z = |z| + i\delta$, and $\arg z = \pi$ for $z < 0$.

We turn now to the analytic structure of Weinberg amplitudes, which using (40) we write as

$$A(E) \equiv \frac{\eta(E)}{1-\eta(E)} = \frac{2\tilde{M}w(z)}{z - z_p + i\pi\tilde{M}\bar{c}\sqrt{z}f(z) - 2\tilde{M}F(z)}, \quad \text{(E8)}$$

where we have defined $z_p = 4\tilde{M}(E_p - E_{\mathrm{th}})$ and E_p is the bare position of the $Q\bar{Q}$ level. The denominator in (E8) can be rewritten as

$$D(z) \equiv z - z_p + ib\sqrt{z}f(0) - z_p(1-\eta(0)) + n(z), \quad \text{(E9)}$$

where we have used relations:

$$\eta(0) = \frac{w(0)}{E_{\mathrm{th}} - E_p} = -\frac{2\tilde{M}w(0)}{z_p},$$

since $w(0) = F(0)$, and $\eta(0) = -\frac{2\tilde{M}F(0)}{z_p}$. We also defined

[4]This is always possible in our Gaussian ansatz for wave functions and subsequent Fourier transform $J(p)$, in a more general case one continues the absorptive part, as it is used in the dispersion relation technic, via the relation $\mathrm{Abs}(f(E)) = \frac{1}{2i} \times (f^{\mathrm{I}}(E) - f^{\mathrm{II}}(E))$, where $f^i(E)$ is the analytic function defined on the ith Riemann sheet. In the general case one might encounter potential type singularities in complex plane, separated from the positive real axis

$b = \pi\tilde{M}\,\bar{c} = \frac{\tilde{M}^2}{\pi}$, and

$$n(z) = ib\sqrt{z}(f(z) - f(0)) - 2\tilde{M}(F(z) - F(0)).$$

Since $n(0) = 0$, we expect it does not affect strongly the analytic structure of $D(z)$ near $z = 0$, where $n(z)$ can be written as

$$n(z) = c_1 z + id_1 z^{3/2} + \mathcal{O}(z^2, z^{5/2}). \tag{E10}$$

The poles of $A(E)$ in the zeroth approximation ($n \equiv 0$) are easily found, denoting $\sqrt{z} \equiv k$; one has two poles at $k = k_+, k_-$, with

$$k_+ = -\frac{ibf(0)}{2} + \sqrt{-\left(\frac{bf(0)}{2}\right)^2 + z_p(1 - \eta(0))}, \tag{E11}$$

$$k_- = -\frac{ibf(0)}{2} - \sqrt{-\left(\frac{bf(0)}{2}\right)^2 + z_p(1 - \eta(0))}. \tag{E12}$$

Here two limiting situations occur: (i) z_p is small (the bare pole is in the proximity of the threshold), or

$$z_p(1 - \eta(0)) \ll \left(\frac{bf(0)}{2}\right)^2. \tag{E13}$$

(ii) z_p is large (pole E_p far from threshold)

$$|z_p(1 - \eta(0))| \gg \left(\frac{bf(0)}{2}\right)^2. \tag{E14}$$

In case (i) the poles are (neglecting higher order terms)

$$k_+ = -i\frac{z_p(1 - \eta(0))}{bf(0)}, \tag{E15}$$

$$k_- = -ibf(0) + i\frac{z_p(1 - \eta(0))}{bf(0)}. \tag{E16}$$

One can see that for weak CC interaction, when $\eta(0) < 1$, both poles are on the second sheet (virtual states), while for strong CC interaction, $\eta(0) > 1$, the pole k_+ is a bound state, while k_- is a virtual state.

Now for case (ii) one can write

$$k_\pm = \pm\sqrt{z_p(1 - \eta(z))}\left(1 - \frac{1}{2}\left(\frac{bf(0)}{2}\right)^2 \frac{1}{z_p(1 - \eta(0))}\right) - \frac{ibf(0)}{2} \tag{E17}$$

and in the standard situation, when $z_1(1 - \eta(0)) > 0$, one has a pair of Breit-Wigner poles $E_0 \mp \frac{i\Gamma}{2}$, with

$$E_0 = E_1(1 - \eta(0)) - \left(\frac{bf(0)}{2}\right)^2 \frac{1}{\tilde{M}}, \tag{E18}$$

$$\Gamma = \frac{p_p\tilde{M}}{\pi} f(0), \qquad p_p = \sqrt{2\tilde{M}(E_p - E_{\text{th}})}. \tag{E19}$$

Note that (E19) coincides with (13) as it should. Using (E8) and (E10) one can write the following analytic representation for the Weinberg amplitude in terms of variable $k \equiv \sqrt{z}$

$$A(k) = \frac{2\tilde{M}(-\frac{i\pi\bar{c}}{2} kf(k^2)) + F(k^2)}{(k - k_+)(k - k_-) + c_1 k^2 + id_1 k^3 + \mathcal{O}(k^4)}. \tag{E20}$$

Note that for the CC poles (k_+, k_- near threshold) the form of $A(k)$ is far from the Breit-Wigner type and is of the cusp type, with infinite energy derivative near the pole, which possibly explains the very narrow peak of $X(3872)$.

Finally, we discuss the case of several thresholds, e.g. in $X(3872)$ for isospin zero one has a sum of $D_0\bar{D}_0^*$ + H.c. and $D_+\bar{D}_-^*$ + H.c. terms in w, so that in the general case one can write for n thresholds:

$$w(E) = \sum_{i=1}^{N} \frac{\bar{c}_i}{2} \int_0^\infty \frac{\sqrt{u}du f_i(u)}{z_i - u}, \tag{E21}$$

where $z_i = 2\tilde{M}_i(E - E_{\text{th}}^{(i)})$. One can apply to $w(E)$ the same procedure as before to separate out nonanalytic terms, with the result that $D(z)$ now has the form

$$D(z) = z - z_p + ib_1\sqrt{z} f_1(0) + i\sum_{i=2}^{n} b_i\sqrt{z - \Delta_i} f_i(-\Delta_i) + n(z), \tag{E22}$$

where we have kept notations for z with respect to the lowest threshold, and $\Delta_i = 2\tilde{M}_i(E_{\text{th}}^{(i)} - E_{\text{th}}^{(1)})$.

It is important that for $z < \Delta_i$ the argument of the square root term is $(i\frac{\pi}{2})$ leading to some renormalization of the term z_p for large Δ_i, while for small Δ_i the situation is complicated and should be solved explicitly in the complex plane z.

[1] E. Eichten, K. Gottfried, T. Kinoshita, K. D. Lane, and T.-M. Yan, Phys. Rev. D **21**, 203 (1980); **17**, 3090 (1978); Phys. Rev. Lett. **36**, 500 (1976).

[2] P. Geiger and N. Isgur, Phys. Rev. D **47**, 5050 (1993); Phys. Rev. Lett. **67**, 1066 (1991); Phys. Rev. D **44**, 799 (1991); **41**, 1595 (1990).

[3] E. van Beveren, G. Rupp, T. A. Rijken, and C. Dullemond, Phys. Rev. D **27**, 1527 (1983); E. van Beveren, C. Dullemond, and G. Rupp, Phys. Rev. D **21**, 772 (1980).
[4] N. A. Tornqvist, Z. Phys. C **68**, 647 (1995); N. A. Tornqvist and M. Roos, Phys. Rev. Lett. **76**, 1575 (1996).
[5] A. M. Badalian, L. P. Kok, M. I. Polikarpov, and Y. A. Simonov, Phys. Rep. **82**, 31 (1982).
[6] Y. S. Kalashnikova, Phys. Rev. D **72**, 034010 (2005); V. Baru, J. Haidenbauer, C. Hanhart, Y. Kalashnikova, and A. E. Kudryavtsev, Phys. Lett. B **586**, 53 (2004).
[7] T. Barnes and E. S. Swanson, Phys. Rev. C **77**, 055206 (2008).
[8] M. R. Pennington and D. J. Wilson, Phys. Rev. D **76**, 077502 (2007).
[9] A. Y. Dubin, A. B. Kaidalov, and Y. A. Simonov, Phys. At. Nucl. **56**, 1745 (1993); A. M. Badalian, A. V. Nefediev, and Y. A. Simonov, Phys. Rev. D **78**, 114020 (2008).
[10] H. G. Dosch, Phys. Lett. B **190**, 177 (1987); H. G. Dosch and Y. A. Simonov, Phys. Lett. B **205**, 339 (1988); Y. A. Simonov, Nucl. Phys. **B307**, 512 (1988).
[11] A. Di Giacomo, H. G. Dosch, V. I. Shevchenko, and Y. A. Simonov, Phys. Rep. **372**, 319 (2002).
[12] A. M. Badalian and I. V. Danilkin, Phys. At. Nucl. **72**, 1206 (2009); A. M. Badalian, A. I. Veselov, and B. L. G. Bakker, J. Phys. G **31**, 417 (2005); A. M. Badalian, B. L. G. Bakker, and I. V. Danilkin, Phys. At. Nucl. **72**, 638 (2009); A. M. Badalian and B. L. G. Bakker, Phys. At. Nucl. **70**, 1764 (2007).
[13] Y. A. Simonov, Phys. At. Nucl. **71**, 1048 (2008).
[14] Y. A. Simonov and A. I. Veselov, Phys. Rev. D **79**, 034024 (2009).
[15] Y. A. Simonov and A. I. Veselov, Phys. Lett. B **671**, 55 (2009).
[16] Y. A. Simonov and A. I. Veselov, JETP Lett. **88**, 5 (2008).
[17] T. Barnes, S. Godfrey, and E. S. Swanson, Phys. Rev. D **72**, 054026 (2005); T. Barnes and E. S. Swanson, Phys. Rev. D **46**, 131 (1992).
[18] E. S. Ackleh, T. Barnes, and E. S. Swanson, Phys. Rev. D **54**, 6811 (1996).
[19] L. Micu, Nucl. Phys. **B10**, 521 (1969); A. Le Yaouanc, L. Oliver, O. Pene, and J. C. Raynal, Phys. Rev. D **8**, 2223 (1973); Phys. Lett. **71B**, 397 (1977); **72B**, 57 (1977).
[20] S. Weinberg, Phys. Rev. **131**, 440 (1963); R. G. Newton, J. Math. Phys. (N.Y.) **1**, 319 (1960); F. Smithies, *Integral Equation* (Cambridge University Press, New York, 1958).
[21] I. M. Narodetsky, Riv. Nuovo Cimento Soc. Ital. Fis. **4**, 1 (1981); Yad. Fiz. **9**, 1086 (1969); A. Herzenberg and F. Mandl, Phys. Lett. **6**, 288 (1963); M. G. Fuda, Phys. Rev. **174**, 1134 (1968).
[22] K. Abe *et al.*, Phys. Rev. Lett. **98**, 082001 (2007); G. V. Pakhlova, arXiv:0810.4114; C.-Z. Yuan (Belle Collaboration), arXiv:0910.3138.
[23] A. M. Badalian, B. L. G. Bakker, and Y. A. Simonov, Phys. Rev. D **75**, 116001 (2007).
[24] S. Hashimoto *et al.*, Phys. Rev. D **61**, 014502 (1999); D. Becirevic *et al.*, Nucl. Phys. **B705**, 339 (2005); D. Brommel *et al.* (QCDSF Collaboration), Proc. Sci., LAT2007 (2007) 364; K. C. Bowler *et al.* (UKQCD Collaboration), Phys. Rev. D **54**, 3619 (1996).
[25] A. M. Badalian, B. L. G. Bakker, and I. V. Danilkin, Phys. Rev. D **79**, 037505 (2009); Phys. At. Nucl. **73**, 138 (2010); A. M. Badalian, A. I. Veselov, and B. L. G. Bakker, Phys. Rev. D **70**, 016007 (2004).
[26] A. M. Badalian and B. L. G. Bakker, Phys. Rev. D **66**, 034025 (2002).
[27] Y. S. Kalashnikova, A. V. Nefediev, and Y. A. Simonov, Phys. Rev. D **64**, 014037 (2001); A. M. Badalian, Y. A. Simonov, and M. A. Trusov, Phys. Rev. D **77**, 074017 (2008); A. M. Badalian, B. L. G. Bakker, and I. V. Danilkin, arXiv:0911.4634.
[28] Y. A. Simonov, Phys. Lett. B **515**, 137 (2001); A. Di Giacomo and Y. A. Simonov, Phys. Lett. B **595**, 368 (2004).
[29] Y. A. Simonov, "Lisbon 1999, QCD: Perturbative or Nonperturbative?".
[30] H. Feshbach, Ann. Phys. (Leipzig) **19**, 287 (1962).
[31] W. M. Yao *et al.* (Particle Data Group), J. Phys. G **33**, 1 (2006).
[32] B. Aubert *et al.* (*BABAR* Collaboration), Phys. Rev. D **79**, 092001 (2009).
[33] Y. S. Kalashnikova and A. V. Nefediev, Phys. Rev. D **80**, 074004 (2009).